Senile plaques in Alzheimer's disease arise from Cathepsin D and Aβ-enriched proteinaceous mixtures out of hemolysis and vascular degeneration

Running title：The blood and vascular origin of senile plaques

Hualin Fu[1, 2*], Jilong Li[1], Peng Du[3], Weilin Jin[1, 2, §], Guo Gao[1, 2], Daxiang Cui[1, 2]

Affiliations:

[1] Institute of Nano Biomedicine and Engineering, Department of Instrument Science and Engineering, School of Electronic Information and Electrical Engineering, Shanghai Jiao Tong University, 800 Dongchuan Road, Shanghai, 200240, P. R. China

[2] National Center for Translational Medicine, Shanghai Jiao Tong University, 800 Dongchuan Road, Shanghai, 200240, P. R. China

[3] Department of Colorectal Surgery, Xinhua Hospital, School of Medicine, Shanghai Jiao Tong University, Shanghai, China

[§] Current address: Institute of Cancer Neuroscience, Medical Frontier Innovation Research Center, The First Hospital of Lanzhou University, The First Clinical Medical College of Lanzhou University, Lanzhou 730000, China

*Correspondence to: hfu@sjtu.edu.cn or 1010720220@qq.com (Hualin Fu)

Abstract

The senile plaque is a prominent pathological hallmark of Alzheimer's disease (AD)，yet the mechanism governing senile plaque generation remains intensively debated. Many researchers believed that senile plaques are derived from neuronal cells; however, there is also strong evidence that senile plaques are linked to cerebral microhemorrhage. We analyzed major neural markers, blood vessel and blood markers on AD brain sections with immunohistochemistry, TUNEL assay, fluorescence imaging and histochemical staining. We found little co-expression between neural markers and

plaque Aβ while abundant co-expression between blood markers such as HBA, HbA1C or ApoE and plaque Aβ. Senile plaques additionally colocalized with a characteristic blue autofluorescence, which also prominently existed in red blood cells. Moreover，platelets were found along blood vessel walls and in plaques, suggesting that platelets also contribute to senile plaque formation. Senile plaque formation was intrinsically linked to vascular degeneration as showed by ColIV, ACTA2 and LRP1 immunostaining. We found that Aβ distributes unevenly among red cells or in the blood vessels, enriching in domains of red cell damage or vascular damage, and with the presence of luminal Cathepsin D expression. In addition，the senile plaques have a constitutive Cathepsin D expression overlapping with Aβ, HBA and HbA1C, reiterating a senile plaque connection with hemolysis. With Rhodanine staining, we further proved that there is widespread hemolysis in AD brain tissues, which concurs with Aβ aggregation, Cathepsin D and ApoE expression. Moreover, we provided the biochemical evidence that Aβ directly interacts with hemoglobin (Hb) and form protease-sensitive complexes in an *in vitro* polymerization assay. In summary, our data suggested that senile plaques arise from Cathepsin D and Aβ-enriched proteinaceous mixtures out of hemolysis and vascular degeneration. In addition, hemoglobin could be a primary physiological target of Aβ in hemolysis and in senile plaques.

Keywords: senile plaque; Aβ; Cathepsin D; hemolysis; vascular degeneration；hemoglobin; Alzheimer’s disease

Introduction

Alzheimer's disease has several important pathological hallmarks such as senile plaques, dystrophic neurites, neurofibillary tangles and cerebral amyloid angiopathy (CAA)[1-4]. Beta amyloid peptide (Aβ) turned out to be a major component in both senile plaques and CAA[5,6]. However, the mechanism governing Aβ generation in senile plaques and the linkage between CAA and senile plaques is still not clear. Most researchers believed that senile plaques are derived from neuronal cells as proposed in amyloid cascade

hypothesis[7,8]. On the other hand, there is also strong evidence showing that senile plaques are linked with cerebral microhemorrhage[9-18]. In depth AD mouse model studies based on bone marrow transplantation experiments also indicated that there is a clear role of hematopoietic cell Aβ contributing to senile plaque development[19]. We used immunohistochemistry, fluorescence imaging, TUNEL assay and histochemical staining to examine the neural, vascular or blood Aβ contribution to senile plaque development in AD brain tissues. We found that there is a lack of significant direct neural cell Aβ input to senile plaques. The true direct source of senile plaque Aβ appears to be Aβ-associated hemolytic red blood cells that come out of cerebral blood vessels through vascular leakage or vascular degeneration while CAA is an important intermediate stage during this senile plaque formation process.

MATERIAL AND METHODS

Tissue sections. AD patient frontal lobe brain paraffin tissue sections were purchased from GeneTex (Irvine, CA, USA). Additionally, AD patient frontal lobe brain paraffin tissue sections were provided by National Human Brain Bank for Development and Function, Chinese Academy of Medical Sciences and Peking Union Medical College, Beijing, China. This study was supported by the Institute of Basic Medical Sciences, Chinese Academy of Medical Sciences, Neuroscience Center, and the China Human Brain Banking Consortium. All procedures involving human subjects are done in accord with the ethical standards of the Committee on Human Experimentation in Shanghai Jiao Tong University and in Xinhua Hospital, and in accord with the Helsinki Declaration of 1975.

List of antibodies for immunohistochemistry. The following primary antibodies and dilutions have been used in this study: Aβ (Abcam ab201061, 1:200), Aβ/AβPP (CST #2450, 1:200), phos-TAU (Abcam ab151559, 1:200), αSyn (Proteintech 10842-1-AP,

88 1:200), MAP2 (Proteintech 17490-1-AP, 1:200), GFAP (Abcam ab33922， 1:200),
89 GFAP (Proteintech 60190-1-Ig, 1:100), Iba1 (Abcam ab178847, 1:200), ColIV (Abcam
90 ab236640, 1:200), ACTA2 (Proteintech 23081-1-AP, 1:400), LRP1 (Abcam ab92544,
91 1:200), ApoE (Abcam ab183597, 1:200), CD42b (Abcam ab210407, 1:200), HBA
92 (Abcam ab92492, 1:200), Anti-Glycophorin A antibody (Abcam ab129024, 1:200),
93 Cathepsin D (Proteintech 66534-1-Ig, 1:100), Cathepsin D (Abcam ab75852, 1:200),
94 HbA1c (OkayBio K5a2, 1:100). The following secondary antibodies and dilutions have
95 been used in this study: donkey anti-mouse Alexa-594 secondary antibody (Jackson
96 ImmunoResearch 715-585-150, 1:400), donkey anti-rabbit Alexa-488 secondary
97 antibody (Jackson ImmunoResearch 711-545-152, 1:400), donkey anti-rabbit Alexa-
98 594 secondary antibody (Jackson ImmunoResearch 711-585-152, 1:400), and donkey
99 anti-mouse Alexa-488 secondary antibody (Jackson ImmunoResearch 715-545-150,
100 1:400).
101
102 **Immunohistochemistry** was performed as described[20]. Briefly, paraffin sections were
103 deparaffinized by Xylene, 100% EtOH, 95% EtOH, 75% EtOH, 50% EtOH, and PBS
104 washes. Sections were treated with 10 mM pH6.0 sodium citrate or 10mM pH9.0 Tris-
105 EDTA solution with microwave at high power for 3 times of 4 minutes, with 5 minutes
106 intervals. The sections were allowed to naturally cool down to room temperature. Then,
107 the slides were blocked with TBST 3%BSA solution for 1 hour at room temperature.
108 After blocking, the samples were incubated with primary antibodies at room
109 temperature for 2 hrs followed by 5 washes of TBST. After that, the samples were
110 incubated with fluorescent secondary antibodies overnight at 4 degree. The treated
111 samples were washed again with TBST 5 times the second day and mounted with
112 PBS+50% glycerol supplemented with H33342 nuclear dye (Sigma, B2261, 1 μg/ml)
113 and ready for imaging. To differentiate nuclear staining from MetaBlue
114 autofluorescence signal, in some of the IHC experiments, PI (Sigma, P4170, 10 μg/ml)
115 was used as a red nuclear fluorescence dye instead of H33342, which stained the nuclei
116 with blue fluorescence. IHC experiments without primary antibodies were used as
117 negative controls. All experiments have been repeated in order to verify the

118 reproducibility of the results.

119

120 **TUNEL assay**. TUNEL assay kits (C1089) were purchased from Beyotime
121 Biotechnology (Shanghai, China). TUNEL assay was performed as described in the
122 manufacturer's user manual. Briefly, paraffin sections were deparaffinized by Xylene,
123 100% EtOH, 95% EtOH, 75% EtOH, 50% EtOH, and H_2O washes. Then, the sections
124 were digested with Proteinase K (20 μg/ml) in 10mM TE buffer (pH 7.5) for 15 minutes
125 at room temperature. After Proteinase K digestion, the slides were washed with PBS
126 for 5 times. The slides were then incubated in 50 μl freshly-prepared TUNEL labeling
127 mixture, covered with parafilm and incubated for 1 hour at 37 degree. Afterwards, the
128 slides were washed with PBS for 5 times and mounted with PBS+50% glycerol solution
129 with Hoechst nuclear dye and examined under fluorescent microscopes. To perform
130 double labeling of TUNEL and antibody staining, the incubation time of Proteinase K
131 treatment was shortened and adjusted to allow the simultaneous detection of protein
132 antigens and TUNEL signals.

133

134 **Rhodanine staining**: The Rhodanine staining kit (BA4346) was purchased from Baso
135 Diagnostics Inc. (Zhuhai, China). Briefly, paraffin sections were first deparaffinized by
136 Xylene, 100% EtOH, 95% EtOH, 75% EtOH, 50% EtOH, and H_2O washes. After a
137 quick wash in 95% ethanol, the slides were stained in the Rhodanine staining solution
138 (0.01% p-Dimethylaminobenzalrhodanine) at 37 degree for 30 minutes. After staining,
139 the slides were treated with a 95% ethanol quick wash and 5 times wash in water, then
140 mounted with PBS+50% glycerol solution for imaging analysis.

141

142 **Slide-based Aβ aggregation assay:** Human Aβ40 or Aβ42 peptides (Apeptide Co.,
143 Shanghai, China) were first solubilized with DMSO at 1 mg/mL concentration. Human
144 hemoglobin (H7379, Sigma) was solubilized in sterile H_2O at 10 mg/mL concentration.
145 Then, Aβ peptides were diluted into sterile PBS solution at 5μM concentration with or
146 without 1.25 μM hemoglobin. The mixture was incubated at 37 degree up to 3 days.
147 Samples were obtained at Day 0, Day 1, Day 2, and Day 3. 2 μl out of each obtained

148 sample was spotted onto adhesive glass slides and dried up in a 37-degree incubator.
149 The glass slides with samples were fixed with 4% formaldehyde in PBS for 10 minutes
150 at room temperature and washed 3 times with PBS. To test the sensitivity of aggregates
151 to protease digestion, paralleled slides were treated with Proteinase K at 20 μg/mL in
152 10mM TE (pH 7.5) buffer for 15 minutes at room temperature. The procedure to
153 analyze the Aβ aggregates on the slides using antibodies was the same as in
154 immunohistochemistry.
155
156 I**maging and morphometry analysis**. Most images were taken with a Leica DM6000B
157 microscope (Leica Microsystems, Wetzlar, Germany) with A4, L5 and N3 fluorescent
158 filter cubes. The microscope is equipped with 10X eyepiece, and 5X, 10X, 20X, 40X
159 objective lens. During the time of manuscript preparation, an Olympus IX71
160 fluorescent microscope (Olympus Co., Toyoko, Japan) was also used to examine the
161 slides. Some additional images were taken by a Keyence BZ-X800 microscope
162 (Keyence Co., Itasca， USA). When comparing marker immunostaining densities,
163 identical exposure settings for fluorescent channels were used for both control and test
164 groups. Images were then analyzed with Image J software. Mean area density was used
165 as the parameter to define the marker densities. The areas of different structures were
166 also measured with Image J software. The total area intensity was calculated by
167 multiplying the area mean density with the measured area. When using the average
168 neural cell as a reference, the values of other anatomical structures divided the mean
169 value of neural cells to obtain the fold numbers. The folds of changes were then
170 expressed as means with standard deviations.
171
172 **Statistics**. All data first went through a Shapiro & Wilk normality test using SPSS
173 Statistics 19 software. Two-tailed unpaired T-test was used to compare the means of
174 data with a normal distribution with Excel 2007 software. For data that were not
175 normally distributed, nonparametric Mann/Whitney test was performed to compare the
176 means with Megastat addin version 10.2. The p Value threshold for statistical
177 significance is set at 0.05. If $p<0.05$, then the difference was considered statistically

178 significant. When $p<0.001$, it was labeled as $p<0.001$. If $p \geqq 0.001$, then the p Value was
179 shown as it was. "*" in the statistical figures indicated the differences are statistically
180 significant.
181
182 **Results:**
183
184 **Neural marker staining rarely overlapped with senile plaque Aβ staining**
185
186 If senile plaque Aβ comes from neural cells, theoretically, senile plaque Aβ expression
187 should overlap with some neural markers because *in vivo* Aβ does not exist as a single
188 species molecule but rather associates with many other molecules[21]. We checked the
189 expression of neuronal marker MAP2, pan-neural marker αSYN and phos-Tau,
190 astroglial marker GFAP and microglial marker Iba1 in AD patient frontal lobe brain
191 tissues. In this study, in order to get a broad image of Aβ-related changes during senile
192 plaque development, "Aβ" refer to all peptides containing the "Aβ" peptide sequence,
193 including the precursor protein AβPP. We found rare overlaps between senile plaque Aβ
194 with MAP2, αSYN and phos-Tau (Figure 1A-F) and some spotty overlaps of GFAP or
195 Iba1 with senile plaque Aβ (Figure 1G-J). Overall, there is no prominent neural marker
196 overlapping with senile plaque Aβ expression. Especially, in the center of dense-core
197 senile plaques, there is no expression of any of the neural markers that we have checked.
198 The data suggested that Aβ from other sources likely form the bulk of Aβ materials in
199 the senile plaques.
200
201 Although neural marker labeling rarely overlaps with the strong fibrillar Aβ signals in
202 senile plaques， neural cells do express Aβ related peptides at very low levels. This very
203 low level of Aβ expression in neural cells can be detected side by side with strong senile
204 plaque Aβ staining with longer exposure settings (Figure 2). In pathological specimens,
205 we observed that some senile plaques or CAA blood vessels were surrounded by a few
206 weakly-stained Aβ-positive neural cells (Figure 2A, C). However, sometimes Aβ-
207 positive neural cells were not observed in the immediate vicinity of senile plaques or

208 CAA blood vessels (Figure 2B, D). Neural cell Aβ staining was much weaker than in
209 senile plaques or CAA (Figure 2E). We also observed significant Aβ staining in luminal
210 patches of blood cells (Figure 2F-H). In order to estimate the relative contribution of
211 Aβ to senile plaques from different sources, we quantitated the densities of Aβ staining
212 in different compartments in the AD brain tissues (Figure 2I, J). We analyzed the mean
213 area Aβ densities of 46 large senile plaques (for simplicity reasons, we only chose a few
214 large senile plaques per view for this analysis), 9 CAA blood vessels, 9 blood vessel
215 luminal Aβ-positive regions and 238 neural cells across 34 high power (40X)
216 microscopic fields in one set of experiments with Aβ staining. The average area in
217 luminal Aβ-positive blood cell patches, CAA and senile plaques is 44.40 (±53.63),
218 19.03 (±9.20), 4.97 (±2.68) fold of the area of an average Aβ-positive neural cell (Figure
219 2I). Comparing to the mean area intensity of Aβ in neural cells, the mean area intensity
220 of luminal Aβ-positive blood cell patches, CAA and senile plaques is around 1.85
221 (±0.59), 5.59 (±0.74), 5.06 (±0.93) fold of an average neural cell (Figure 2J). The mean
222 area Aβ intensity of CAA was not statistically different from the mean area Aβ intensity
223 of senile plaques ($p=0.08$), while the difference between Aβ intensities of luminal Aβ-
224 positive blood cell patches and average neural cells was statistically significant
225 ($p<0.001$). By multiplying the average area and mean area intensity numbers， the total
226 area intensity of Aβ in an average senile plaque is roughly 25.14 times of the total area
227 Aβ intensity of an average neural cell. Take this estimation to the three-dimensional
228 level, an average senile plaque approximately contains the same amount of Aβ in as
229 many as 126.03 average neural cells (estimated by multiplying the total area intensity
230 fold number with the square root of the total area intensity fold number). In another
231 word, an average Aβ-positive neural cell only has about 0.79% of the Aβ content in an
232 average senile plaque. Based on counting results from 34 high power fields, each
233 microscopic field contained by average 2.62 (±1.99) large senile plaques while 46.94
234 (±9.53) Aβ-positive neural cells. When comparing to an average senile plaque, the mean
235 area Aβ intensities of luminal patches and CAA are 0.37 (±0.12) and 1.10 (±0.15) fold
236 of an average senile plaque. The average areas of luminal patches and CAA are 8.94
237 (±10.8) and 3.83 (±1.85) fold of an average senile plaque. At the three-dimensional

238 level, an average CAA blood vessel contains the same amount of Aβ as in roughly 8.65
239 average senile plaques while an average luminal Aβ-positive region contains the same
240 amount of Aβ as in roughly 6.02 average senile plaques. The experiment was repeated
241 on different samples and with different fluorophores and the results showed similarly
242 the extremely low Aβ expression in neural cells comparing to senile plaques. This
243 quantitative analysis pointed out that the very low level Aβ in neural cells and the
244 limited number of neural cells might not provide sufficient amount of Aβ for the senile
245 plaque formation while Aβ-positive blood cells and CAA blood vessels contained
246 sufficient amount of Aβ, which could be the source of Aβ in senile plaques.

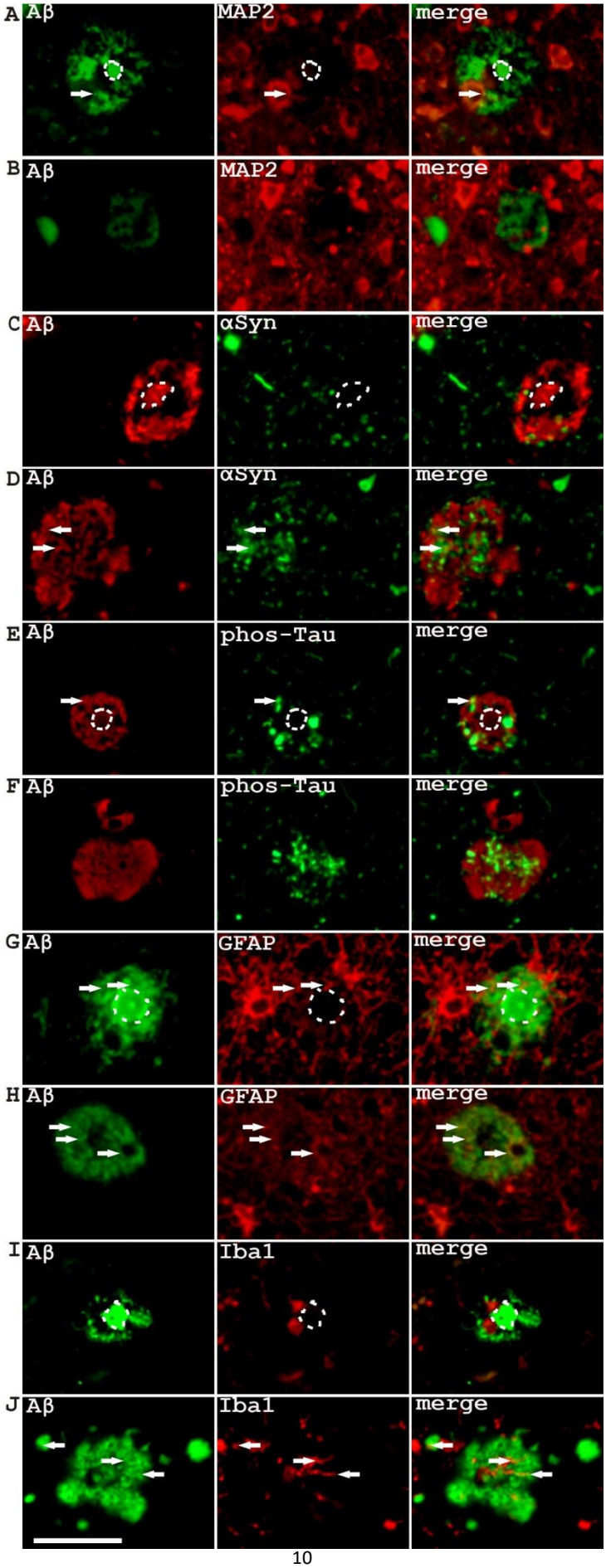
A
Aβ
MAP2
merge
B
Aβ
MAP2
merge
C
Aβ
αSyn
merge
D
Aβ
αSyn
merge
E
Aβ
phos-Tau
merge
F
Aβ
phos-Tau
merge
G
Aβ
GFAP
merge
H
Aβ
GFAP
merge
I
Aβ
Iba1
merge
J
Aβ
Iba1
merge

247

248 **Figure 1. Co-immunostaining of neuronal marker MAP2, pan-neural markers**
249 **αSYN and phos-Tau or glial cell markers GFAP and Iba1 with Aβ in dense-core**
250 **(top panel for each marker) or diffusive senile plaques (bottom panel for each**
251 **marker).** (**A-B**), MAP2; (**C-D**), αSYN; (**E-F**), phos-Tau; (**G-H**), GFAP; (**I-J**), Iba1.
252 Arrows pointed to possible overlapping of the markers. The circled areas indicated the
253 core of dense-core plaques, which were not stained with any of the neural markers
254 examined. Scale bar, 50 μm.
255

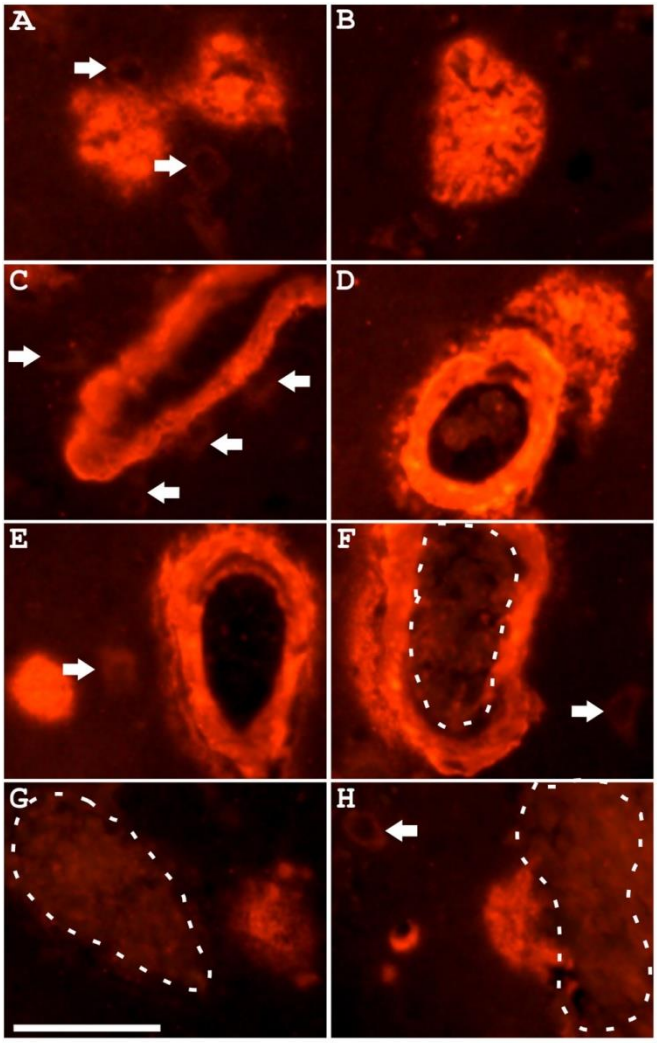
A
B
C
D
E
F
G
H

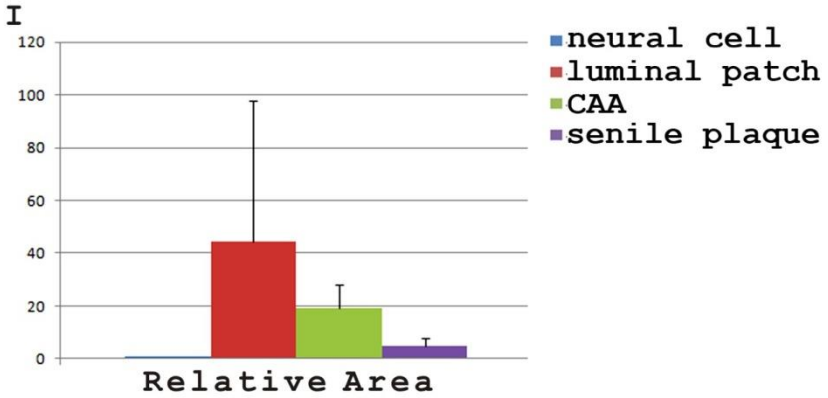
I
120
100
80
60
40
20
0
Relative Area
neural cell
luminal patch
CAA
senile plaque

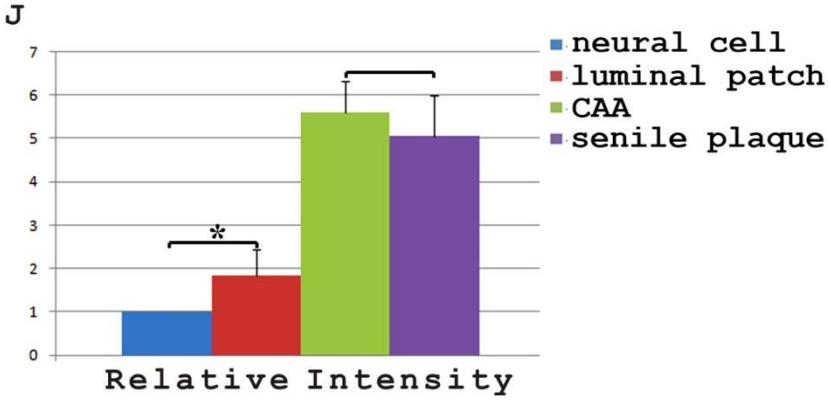
J
7
6
5
4
3
2
1
0
*
Relative Intensity
neural cell
luminal patch
CAA
senile plaque

256

Figure 2. Aβ staining in neural cells, senile plaques, CAA, and luminal patch of Aβ-positive blood cells. (**A**，**B**) Senile plaques with or without weakly Aβ-positive neural cells at the vicinity. (**C**，**D**) CAA with or without weakly Aβ-positive neural cells at the vicinity. **E.** Neural cell Aβ (indicated with an arrow) staining was much weaker comparing to plaque (left) or CAA (right) Aβ staining. **F.** CAA and luminal blood cell Aβ staining was stronger than neural cell Aβ staining (indicated with an arrow). **G.** Blood cell Aβ staining (on the left) intensity was weaker comparing to a developing senile plaque (on the right). **H.** Perivascular plaque and blood cell Aβ staining (dashed lines) was stronger than neural cell Aβ staining (indicated with an arrow). The arrows indicated the weakly stained neural cells. The dashed lines indicate luminal blood cells. Scale bar, 50 μm. **I.** The average area in luminal Aβ-positive blood cell patches, CAA and senile plaques is 44.40±53.63, 19.03±9.20, 4.97±2.68 fold of the area of an average neural cell. **J.** The mean area intensity of luminal Aβ-positive blood cell patches, CAA and senile plaques is around 1.85±0.59, 5.59±0.74, 5.06±0.93 fold of an average neural cell. Aβ intensities of luminal Aβ-positive blood cell patches were significantly higher than average neural cells ($p<0.001$) while no significant difference was detected between CAA and senile plaque Aβ intensities ($p=0.08$). The asterisk indicated statistical significance.

Senile plaque Aβ staining seldom colocalized with nuclear stains

Because Aβ often showed extracellular localizations, people assumed that Aβ might be derived from dead neurons. However, the direct evidence that linked senile plaque Aβ with dying neurons is lacking. In our analysis, most Aβ plaques did not have nuclei associations, agreeing with their predominantly extracellular localizations (Figure 3A). In addition, Aβ plaques did not colocalized with TUNEL-labeled nuclei, disagreeing with the assumption that Aβ might come from dying neurons (Figure 3B). Surprisingly, we observed a faint blue fluorescent staining in the centers of many dense-core plaques, which showed amorphous irregular patterns distinct from densely-stained oval shape nucleus staining (Figure 3A, bottom). To differentiate blue autofluorescence from blue

nuclei staining, we switched to use a red fluorescence nuclei dye Propidium Iodide (PI). We proved that the amorphous blue fluorescent staining in the center of dense-core senile plaques is a blue autofluorescence, but not nuclei staining (Figure 3C). This blue autofluorescence was a robust and consistent marker of senile plaques, which associated with senile plaques of different morphologies and sizes including dense-core senile plaques, large diffusive senile plaques and small diffusive senile plaques (with more pictures shown in Supplementary Figure 1). We think the blue autofluorescent material could be a constitutive component of senile plaques that associates with Aβ during the full course of senile plaque formation process. At the time of preparing this manuscript, we noticed that several earlier studies already recognized senile plaques had characteristic autofluorescence although the true source of this blue autofluorescence is unknown[22,23]. To facilitate the study and discussion on this unique and potentially important substance, we would like to give a temporary special name for this material as "MetaBlue" in this manuscript (meaning for a blue metabolite or a mixture of blue metabolites) until the accurate identity of this material is fully revealed.

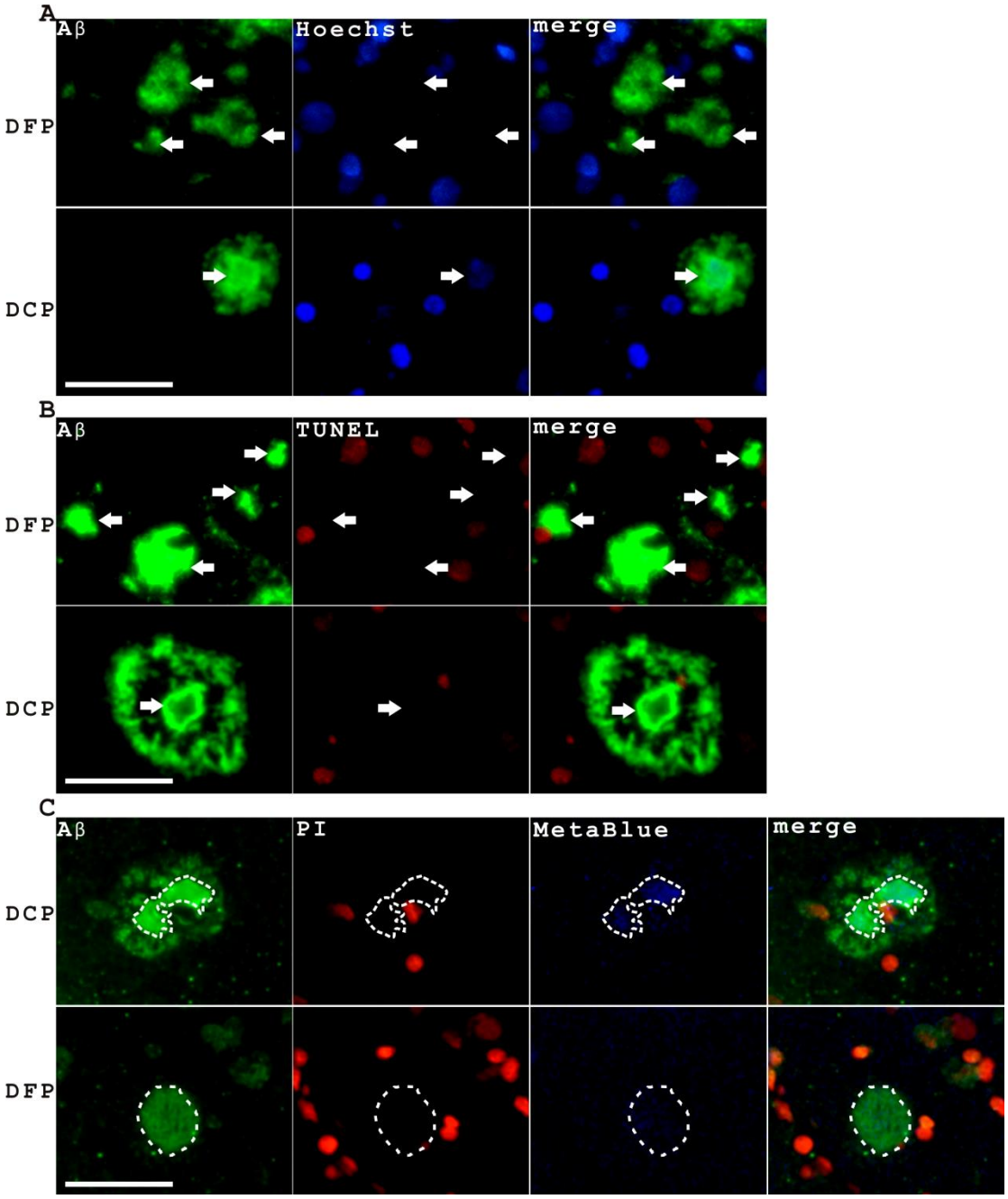

Figure 3. Senile plaques seldom associated with nuclei DNA staining. A. Senile plaques were seldom stained with Hoechst. Diffusive plaques (DFP) or stella plaques were mostly not stained with Hoechst. Irregular amorphous blue fluorescent signals were observed in the cores of dense-core plaques (DCP) but distinct from nuclear staining. Arrows point to senile plaques. **B.** Diffusive plaques (DFP) or dense-core plaques (DCP) were not associated with TUNEL-labeled nuclei. Arrows point to senile plaques. **C.** Dense-core plaques (DCP) had a relatively strong blue autofluorescence while the blue autofluorescence signal in diffusive plaques (DFP) was weak. The

313 dashed lines indicated dense-core or diffusive senile plaques with blue autofluorescence
314 but without PI-positive nuclei. Scale bar, 50 μm.
315
316 **Senile plaque Aβ staining overlapped with MetaBlue, a specific blue**
317 **autofluorescence, that was also prominently found in red blood cells**
318
319 To trace the origin of MetaBlue, we combined immunohistochemistry staining with
320 autofluorescence imaging. We found that MetaBlue was prominently associated with
321 Aβ (Figure 4A) and HBA (Figure 4B) in CAA blood vessel wall， senile plaques and
322 red blood cells. The intensity of MetaBlue in the center of Aβ-marked dense-core
323 plaques is comparable to the MetaBlue intensity in CAA blood vessels and often higher
324 than in diffusive senile plaques, which suggested that MetaBlue is either degraded or
325 dispersed in diffusive plaques or the diffusive plaques have less MetaBlue materials
326 starting with. MetaBlue signals were clearly observed in red blood cells identified with
327 HBA or Glycophorin A staining (Figure 4C). With the senile plaque association of
328 predominantly blood origin MetaBlue and HBA but much less with neural markers such
329 as MAP2, αSYN, phos-TAU, GFAP and Iba1, it suggested that senile plaque Aβ might
330 directly come from the blood instead of neural cells.

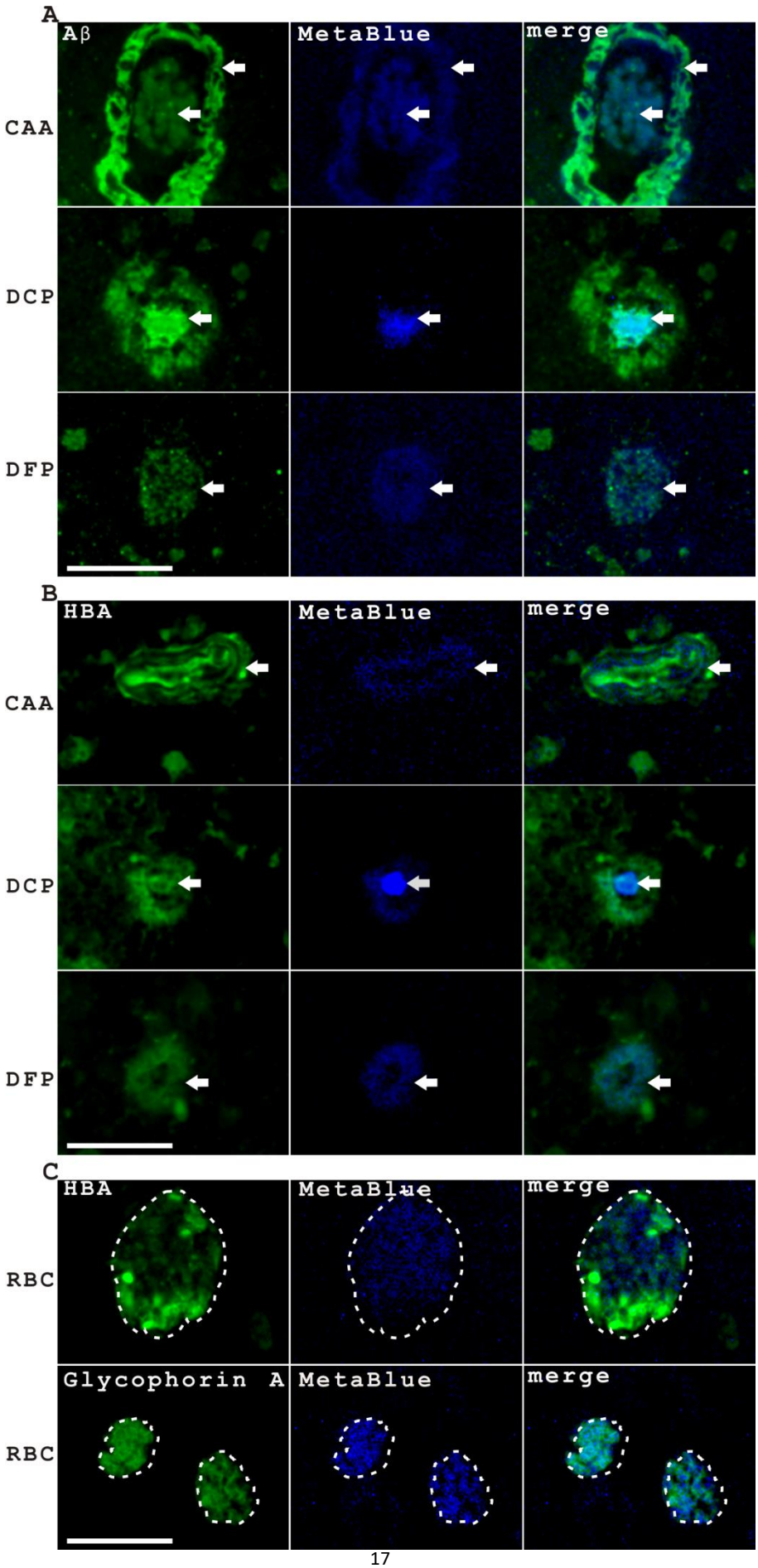
A
Aβ
MetaBlue
merge
CAA
DCP
DFP
B
HBA
MetaBlue
merge
CAA
DCP
DFP
C
HBA
MetaBlue
merge
RBC
Glycophorin A
MetaBlue
merge
RBC

331

332 **Figure 4. The MetaBlue blue autofluorescence signals overlapped with Aβ and**
333 **alpha hemoglobin (HBA) staining in CAA, dense-core plaques and diffusive**
334 **plaques and were also present in the red blood cells. A.** MetaBlue signals co-stained
335 with Aβ in CAA, dense-core plaques (DCP) and diffusive plaques (DFP). **B.** MetaBlue
336 signals co-stained with HBA staining in CAA, dense-core plaques, and diffusive
337 plaques. **C.** MetaBlue signals were clearly observed in red blood cells (RBC) labeled
338 either with HBA or with Glycophorin A. The arrows pointed to the co-expression of
339 markers. Dashed lines indicated red blood cell clusters with overlapping MetaBlue
340 staining. Scale bar, 50 μm.
341
342 **The association of blood markers HBA, HbA1c, ApoE, CD42b with senile plaques**
343
344 To directly check the association of Aβ with blood markers， we did co-staining of Aβ
345 with red blood cell marker HBA and HbA1C (shown in Figure 5), blood plasma marker
346 ApoE and platelet marker CD42b (shown in Figure 6). Aβ staining was observed to
347 associate with HBA staining in CAA, in dense-core plaques and in diffusive plaques
348 (Figure 5A). However, not all senile plaques showed the same intensity HBA staining.
349 In some diffusive plaques, HBA immunostaining signals were very weak (Figure 5A,
350 bottom). The heterogeneity of HBA signals in senile plaques likely reflected the
351 heterogeneous and dynamic nature of senile plaque formation, which was repeatedly
352 observed in our experiments with multiple markers. More pictures showed the red blood
353 cell Aβ staining was provided in Supplementary Figure 2. Since HbA1C is a glycation
354 product of hemoglobin, which is also related to diabetes and aging changes of red blood
355 cells[24], we decided to check the expression of HbA1C in senile plaques. The experiment
356 results indicated that HbA1C staining also associated with Aβ staining in CAA, in
357 dense-core plaques and in diffusive plaques (Figure 5B).
358
359 Since ApoE is a plasma protein that associates with Aβ, which is an important modifier
360 of AD risk[25], it is important to examine the interactions between Aβ and ApoE during
361 senile plaque development. We observed that Aβ staining associated with ApoE in small

362 or large patches in the blood vessel lumens, and also in CAA and perivascular plaques,
363 in dense-core senile plaques and in diffusive senile plaques (Figure 6A). The frequent
364 presence of ApoE in blood vessel lumen suggested that ApoE is mostly derived from
365 the blood (Figure 6A, second and third panels). In addition, ApoE intensity was highly
366 variable in senile plaques while senile plaque Aβ intensity is relatively stable, which
367 again suggested the dynamic nature of senile plaques (Figure 6A, bottom two panels).
368 ApoE associated with senile plaques of different morphologies such as dense-core or
369 diffusive senile plaques and with different sizes regardless they were large or small,
370 with more pictures shown in Supplementary Figure 3. We think that ApoE could be an
371 additional constitutive component of senile plaques besides Aβ and MetaBlue.
372
373 Platelets are another important type of cells in the blood that frequently link to blood
374 abnormalities in many diseases. Platelets was previously thought to be related to senile
375 plaque formation and be an important source of AβPP[26]. We used CD42b as a marker
376 of platelets to analyze the behavior of platelets during senile plaque formation. We
377 found that Aβ-positive and CD42b-positive platelets attached to blood vessel walls,
378 indicating the presence of blood vessel damage as it is well-known that blood vessel
379 wall damage activates platelets and attracts platelets to the damage sites (Figure 6B,
380 top). Large aggregations of CD42b-positive platelets with clearly detectable Aβ
381 expression were also found in the blood vessels, suggesting the happening of
382 intravascular coagulation (Figure 6B, middle). Additionally, CD42b-positive platelets
383 were found in dense-core senile plaques (Figure 6B, bottom). However, the staining
384 intensity of Aβ on platelets was in general lower comparing to what we observed in Aβ-
385 positive red blood cells in AD brain tissues. With complicated regulations between
386 platelets and red blood cells[27-30], platelet could be another significant player involving
387 blood leakage and senile plaque formation.
388

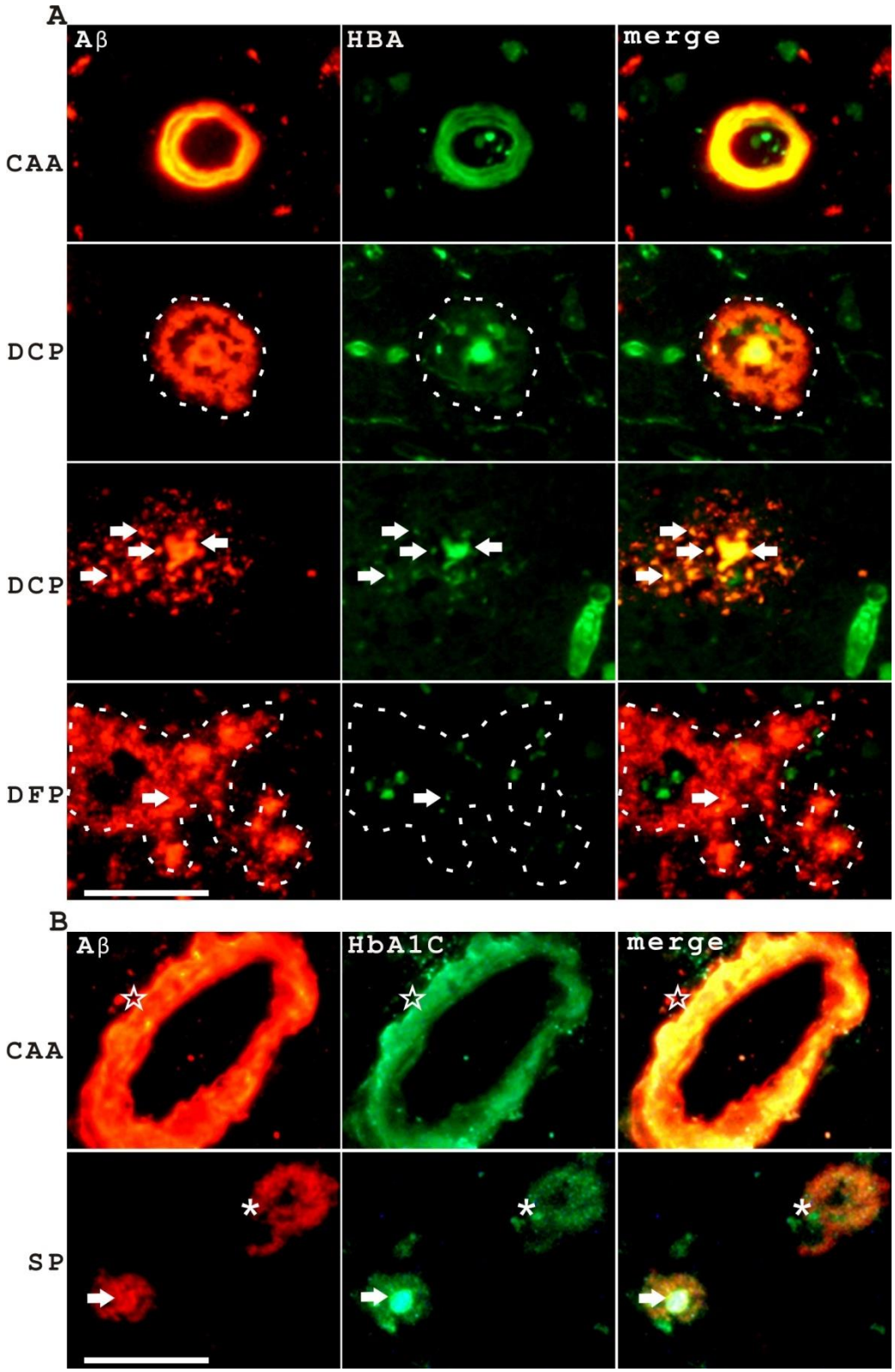

389

390 **Figure 5. Hemoglobin colocalized with Aβ during different stages of senile plaque**
391 **development. A.** Red cell markers HBA co-expressed with Aβ at different stages of
392 senile plaque development, in CAA, dense-core plaques and diffusive plaques.
393 However, not all senile plaques display strong HBA staining. Some large diffusive

394 plaques with very weak HBA staining were also observed (bottom). The dashed lines
395 indicated dense-core senile plaques or diffusive plaques. The arrows indicated some
396 diffusive Aβ aggregates. **B.** Red cell marker HbA1C (glycated hemoglobin）also co-
397 expressed with Aβ in CAA (indicated with pentagons) and dense-core plaques
398 (indicated with arrows) and diffusive plaques (indicated with asterisks). Scale bars, 50
399 μm.
400
401

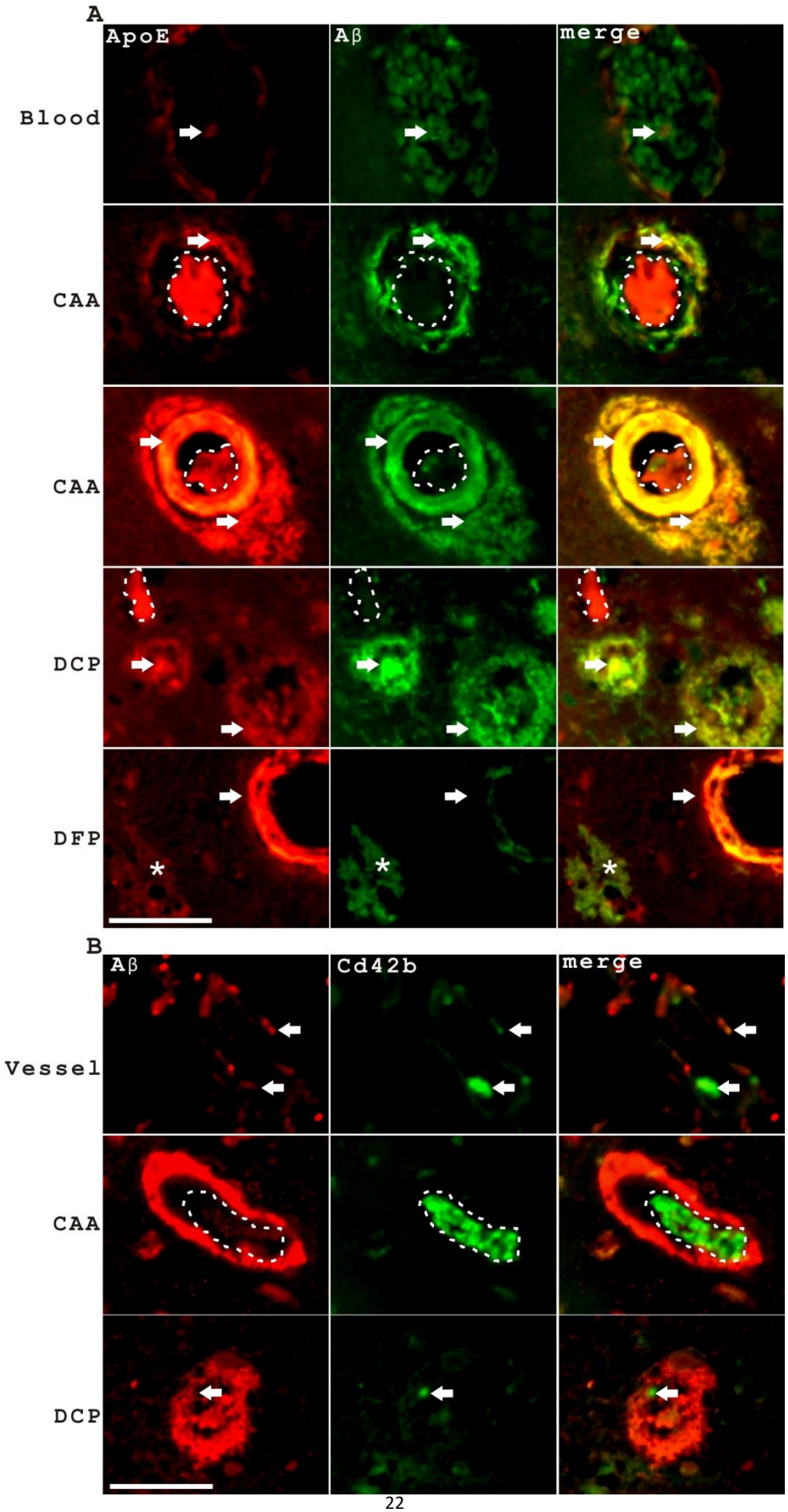
A
ApoE
Aβ
merge
Blood
CAA
CAA
DCP
DFP
*
*
*
B
Aβ
Cd42b
merge
Vessel
CAA
DCP

402

403 **Figure 6. The association of blood marker ApoE and platelet marker CD42b with**
404 **senile plaque development. A.** ApoE associated with Aβ in small blood cell patches in
405 the vessel (top), in large patches in the vessel and in perivascular plaques (second panel),
406 in CAA (third panel), in dense-core senile plaques (fourth panel) and in diffusive
407 plaques (bottom). Arrows indicated the co-expression of markers in CAA and senile
408 plaques. Dashed lines indicated the staining in luminal blood patches. The asterisk
409 indicated a diffusive senile plaque with ApoE staining much weaker than neighboring
410 CAA. **B.** CD42b-labeled platelets participated senile plaque development. Platelets
411 with Aβ expression were observed in platelets adhering to vascular wall (top) or in
412 platelet aggregations in the blood vessel (middle). Platelets were also observed directly
413 in senile plaques (bottom). The arrows indicated the platelets. The dashed lines
414 indicated a patch of aggregated platelets. Scale bars, 50 μm.
415
416 **The dynamic interaction of Aβ expression and vascular degeneration during senile**
417 **plaque development examined with ColIV, ACTA2 and LRP1 staining**
418
419 CAA, vascular degeneration and microhemorrhage have been long implicated to be
420 involved in the senile plaque formation[9,10,12,17,18]. However, the exact contribution of
421 blood vessels to senile plaques is not so clear. We used ColIV as a blood vessel marker
422 to examine the blood vessel changes during the senile plaque formation process (Figure
423 7). As it is well-known, ColIV labels the extracellular matrix collagen component of
424 the blood vessels. Firstly, we observed patches of strong Aβ staining with diffusive
425 luminal ColIV staining in the blood vessels, an indication of blood vessel damage
426 (Figure 7, top). We also observed Aβ staining associates with ColIV staining in vessel
427 walls in CAA (Figure 7, second panel). In CAA blood vessels, some overlapping of Aβ
428 and ColIV staining was observed, suggesting Aβ probably was accumulated in the
429 vessel extracellular matrix. In addition, we observed strong perivascular Aβ staining
430 with concurrent diffusive ColIV staining, again indicating blood vessel damage (Figure
431 7, third panel). Moreover, balloon-shape bulge formation in large blood vessels was
432 also detected (Figure 7, fourth panel). These bulges contained condensed staining of Aβ

433 that was surrounded by degenerative ColIV staining, indicating that blood vessel
434 aneurysm could be formed, which might be a way to induce dense-core senile plaques.
435 This observation is consistent with a previous study stating lumpy and bumpy blood
436 vessels were found in AD brain tissues by using scanning electron microscopy[31]. The
437 tight association between senile plaque formation and vascular degeneration was
438 observed in both dense-core senile plaques (Figure 7, fifth to seventh panel) and
439 diffusive senile plaques（Figure 7, bottom). Our observation suggested that the senile
440 plaque formation is intrinsically linked with vascular degeneration and
441 microhemorrhage with blood-borne Aβ leakage.
442
443

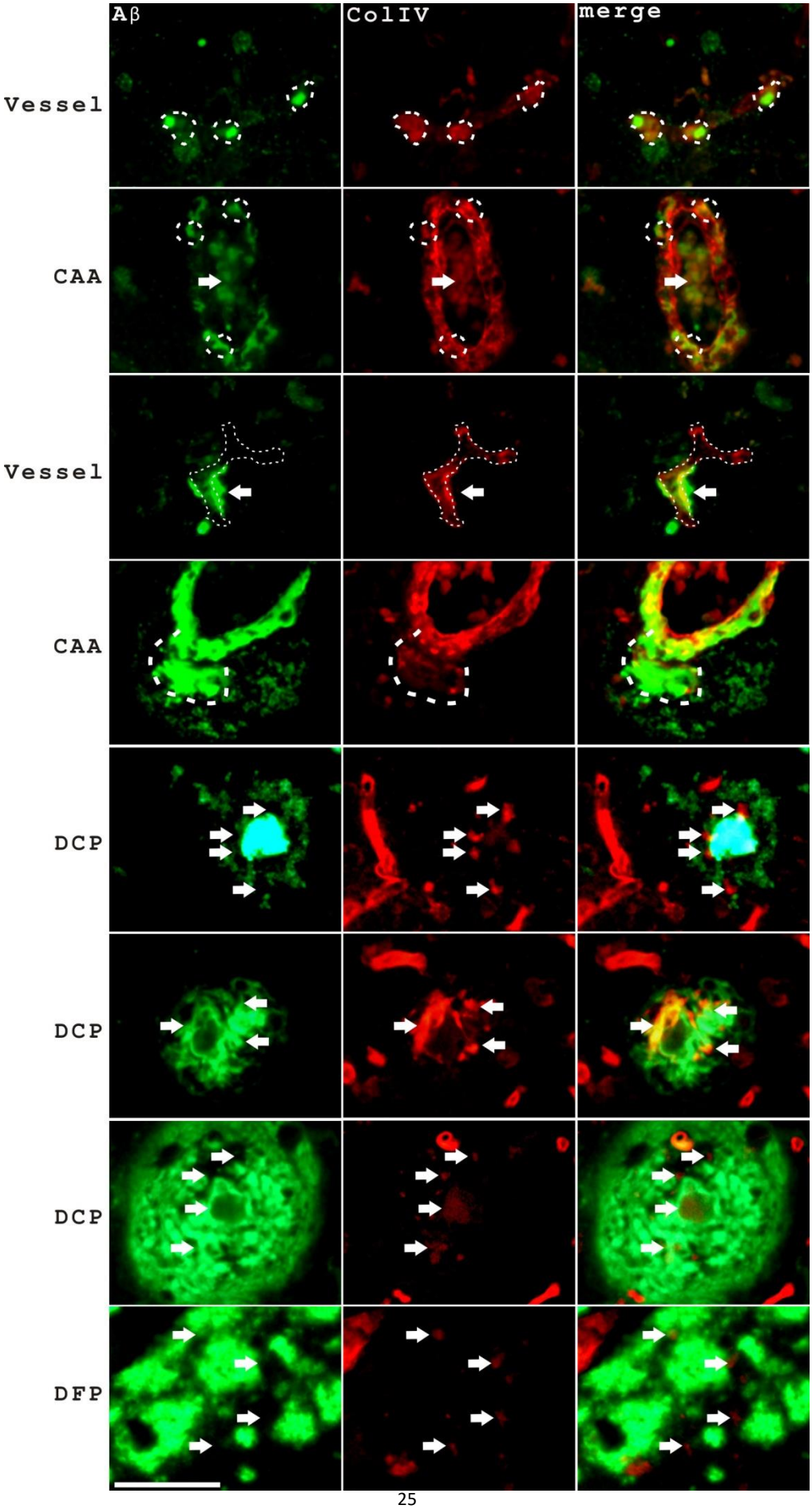

444

445 **Figure 7. The dynamic interaction of Aβ expression and blood vessel alterations in**
446 **senile plaque development.** Discrete condensed Aβ staining was observed in a blood
447 vessel accompanying diffusive ColIV staining in the vessel lumen (indicated by dashed
448 lines in the top panel). Aβ staining associated with CAA blood vessel wall (indicated
449 by dashed circles) and also blood cells (indicated with arrows in the second panel). Aβ
450 perivascular staining (indicated with arrows in the third panel) was associated with a
451 "dissolving" blood vessel phenotype (indicated with dashed lines) with diffusive ColIV
452 staining in the vessel lumen. A bulge-like structure (indicated with dashed lines in the
453 fourth panel) was observed in a large blood vessel containing concentrated Aβ,
454 suggesting blood vessel aneurysm might be happening. Three examples of dense-core
455 senile plaques showed degenerated blood vessel remnants (indicated with arrows in the
456 fifth, sixth, seventh panels) scattering around senile plaque structures. An example of a
457 diffusive senile plaque intermingled with degenerated vessel remnants (indicated with
458 arrows in the bottom panel) was also shown. Scale bar, 50 μm.
459
460 To further illustrate the relationship of vascular defects with senile plaque formation,
461 we also analyzed two other blood vessel related markers ACTA2 and LRP1. ACTA2
462 labels the smooth muscle cells of the blood vessels. LRP1 is an ApoE receptor involving
463 Aβ clearance that expresses strongly in the endothelium of blood vessels[32,33]. Our
464 experiment showed that in early stages of CAA development, ACTA2 staining regions
465 were mostly complementary to Aβ staining regions in the blood vessels, suggesting that
466 the initial Aβ in the CAA blood vessel probably resided in the blood vessel extracellular
467 space (Figure 8A, top). This is consistent with the observations of some overlapped
468 staining between Aβ and ColIV, which is a marker of blood vessel extracellular matrix.
469 These observations hinted that CAA is probably formed by blood leakage through the
470 endothelial cell barrier into blood vessel extracellular matrix. We also observed
471 diffusive staining of ACTA2 in CAA blood vessel lumen and some large diffusive
472 patches of ACTA2 staining in the AD brain tissues (Figure 8A, second and third panels),
473 both of which indicated blood vessel degeneration, similarly as it was shown by
474 diffusive ColIV staining. Additionally, degenerated blood vessel remnants marked with

475 ACTA2 were also observed in the center of senile plaques (Figure 8A, bottom), further
476 confirming the direct relation between senile plaque formation and vascular
477 degeneration.
478
479 LRP1 was observed to label the blood vessels with diffusive luminal staining of Aβ
480 (Figure 8B, top). LRP1 also clearly labeled blood vessel structures surrounding the
481 center of dense-core senile plaques (Figure 8B, middle and bottom). We also observed
482 that condensed Aβ came out of blood vessels precisely on site through openings on the
483 vessel wall (indicated with arrows in Figure 8B, middle and bottom panels). Small
484 vessel degeneration with Aβ in the lumen might be another way to produce dense-core
485 plaques besides blood vessel aneurysm.
486

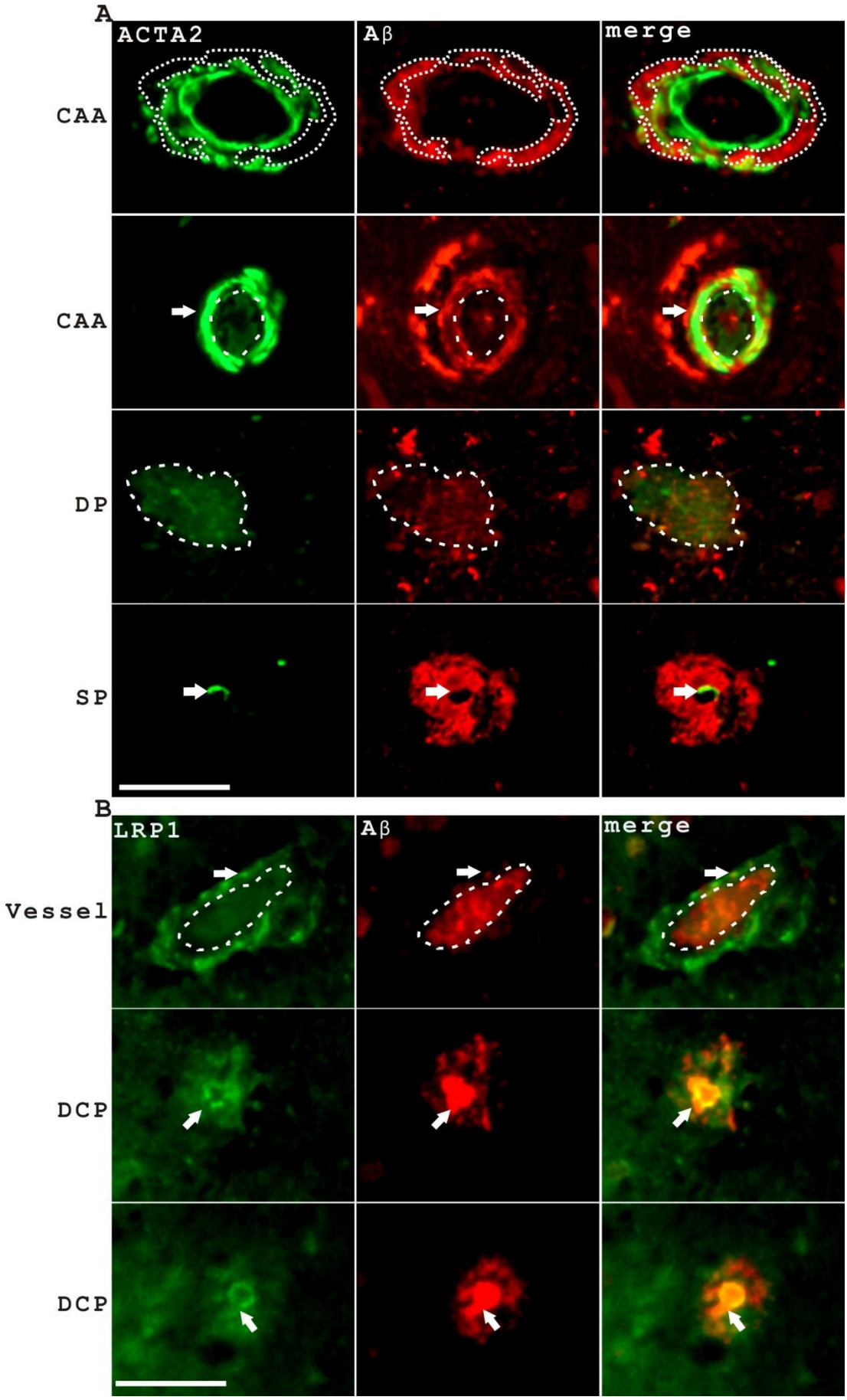

487

488 **Figure 8. The dynamic interaction of Aβ expression and blood vessel marker**
489 **ACTA2 and LRP1 in senile plaque development. A.** The dynamic interaction of Aβ
490 expression and blood vessel marker ACTA2 in senile plaque development. CAA Aβ
491 staining mostly showed a complementary expression pattern relative to ACTA2, a
492 smooth muscle cell marker (indicated with dashed lines in the top panel). ACTA2
493 staining was also observed in the vessel lumen (indicated with dashed lines in the
494 second panel) of a CAA blood vessel (indicated with an arrow). A diffusive patch (DP)
495 of ACTA2 staining, an indication of blood vessel degeneration, was observed to
496 associate with diffusive, fibrillar Aβ staining (indicated with dashed lines in the third
497 panel). Degenerated blood vessel remnants with ACTA2 staining were also observed in
498 the center of a senile plaque (indicated with arrows in the bottom panel). **B.** The
499 dynamic interaction of Aβ expression and blood vessel marker LRP1 in senile plaque
500 development. LRP1 expression was observed in the blood vessel wall, also in the blood
501 vessel structures in the dense-core senile plaques (DCP). The arrows indicated the co-
502 expression of markers. Scale bar, 50 μm.
503
504 **Blood vessel Aβ expression associates with red blood cell damage and vascular**
505 **damage**
506
507 After repeated experiments of Aβ staining in the blood cells and in the blood vessels, it
508 came clear to us that Aβ does not distribute evenly among blood cells or along the blood
509 vessels. It appeared that Aβ was associated with patches of red cells with reduced and
510 diffusive HBA staining, an indication of red blood cell damage or hemolysis (Figure
511 9A, top three panels). Sometimes, specific ring-shape Aβ stained structures were
512 observed in the blood vessels, which associated with red blood cells (Figure 9A,
513 bottom). Aβ staining was stronger in blood vessels with diffusive ColIV staining in the
514 vessel lumens (Figure 9B, top), suggesting an Aβ association with the solubilization
515 and damage of blood vessel structures. Some strongly stained Aβ aggregates began to
516 emerge in the fields of diffusive Aβ staining associated with vascular degeneration with
517 diffusive ColIV staining (Figure 9B, bottom two panels). Thus, the Aβ staining in the

518 blood vessels was closely associated with both red blood cell damage and vascular
519 damage.
520

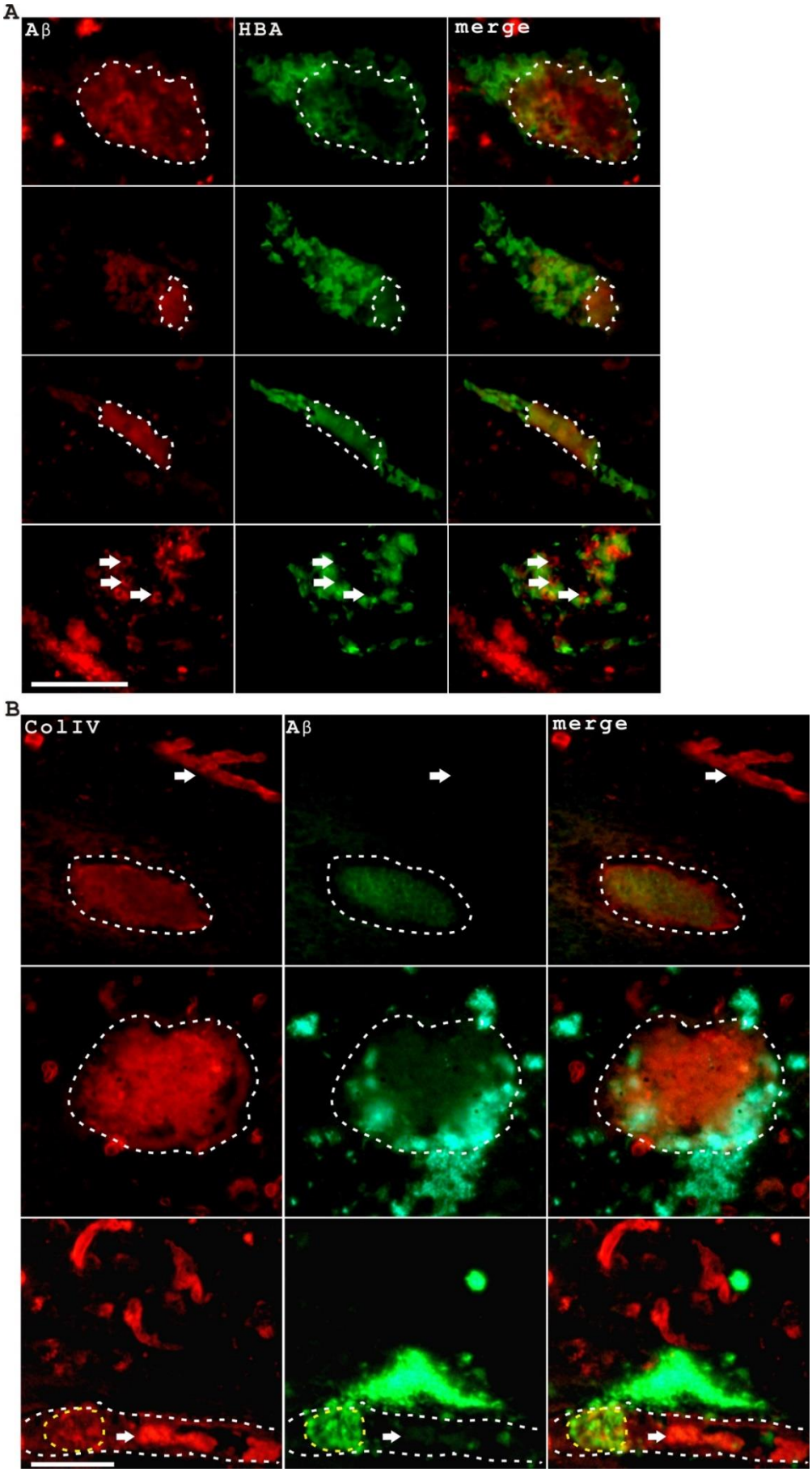

521

522 **Figure 9. Aβ staining in the blood vessels associates with red cell damage and**
523 **vascular damage. A.** Aβ staining in the blood vessels associated with red cell damage.
524 Top three panels showed images indicating the association of Aβ staining with weak
525 and diffusive Hb staining, a sign of red blood cell damage or hemolysis. The bottom
526 panel showed some ring-shape structures with Aβ staining formed closely around red
527 blood cells. **B.** Aβ staining in the blood vessels associated with vessel damage. Aβ
528 staining in a blood vessel with diffusive ColIV staining in the vessel lumen (marked
529 with dashed lines) was compared to a normal looking vessel with clear ColIV vessel
530 outline staining (marked with an arrow in the top panel). A large area of diffusive ColIV
531 and Aβ staining with degenerating vessel walls was observed (marked with dashed lines
532 in the middle panel). Some Aβ aggregations with bright staining also formed within this
533 area. The bottom panel indicated a vessel with collapsed ColIV-positive components in
534 the vessel lumen that intermingled with a strong Aβ staining. Some areas of strong
535 luminal ColIV staining but with weak Aβ staining were also observed. The dashed lines
536 indicated the blood vessel or the diffusive luminal ColIV-positive areas. Scale bar, 50
537 μm.
538
539 **Aβ staining in the blood vessels and the in senile plaques is associated with**
540 **Cathepsin D expression**
541
542 The enhancement of Aβ staining in damaged red blood cells or in the vascular domains
543 with vascular damage could be due to either enhanced expression of Aβ-related peptides
544 or enhanced aggregation of Aβ monomers. Aβ aggregation is depending on both the
545 synthesis of Aβ-related peptides and also the amyloidgenic activity of beta-site cutting
546 enzymes. It is well known that hemolysis or vascular damage can activate platelets,
547 which are able to secrete a large amount of AβPP. As for the beta-site cutting enzymes，
548 besides BACE1, the assumed main beta-site cutting enzyme[34,35], with ongoing debates,
549 many other proteases also have potential beta-site cutting activity, such as Cathepsin
550 D[36-38], Cathepsin B[39,40], Carboxypeptidase B[41] and MMP2[42]. Cathepsin D was associated
551 with AD risk genetically[43,44] and was also found to be present in senile plaques by

552 previous researches[45,46]. In our previous study investigating the relation between
553 lysosomal Cathepsin D and senile plaque development, we unexpectedly found that
554 domains of enhanced Aβ staining in the blood vessels coincided with luminal Cathepsin
555 D expression (Figure 10A, top). Some small but strongly stained Aβ aggregates
556 emerged in the luminal domains with diffusive Cathepsin D expression (Figure 10A,
557 second panel). Additionally, in CAA blood vessels, there existed patches of strong
558 Cathepsin D expression associating with significant Aβ staining (Figure 10A, third
559 panel). It was also clear that CAA blood vessel walls were Cathepsin D-positive. The
560 connection between Cathepsin D and Aβ expression was further strengthened when we
561 extended the investigation into senile plaques (Figure 10B). Very surprisingly, with
562 optimized immunostaining conditions，we observed that senile plaques came with a
563 constitutive Cathepsin D expression. Apparently, in senile plaques, there were two
564 distinct layers of Cathepsin D staining. One layer was a strong, granule type of
565 Cathepsin D staining, typical of lysosomes, which stained complementary locations
566 related to Aβ staining in senile plaques (Figure 10B, first, third and fifth panels).
567 Another type was a weaker and diffusive Cathepsin D expression, which often stained
568 a large portion of senile plaque area and showed overlapping staining with Aβ (Figure
569 10B, second, fourth and sixth panels). This constitutive Cathepsin D staining was often
570 detected in dense-core senile plaques. In diffusive senile plaques, the constitutive
571 Cathepsin D expression was weak, however, still detectable. The heterogeneity of
572 constitutive Cathepsin D intensities in senile plaques is probably due to the dynamic
573 nature of senile plaques, especially because they are self-digestive compartments highly
574 enriched for proteases such as Cathepsin D. The two-layer Cathepsin D expression
575 pattern in the senile plaque was further confirmed with a different Aβ/Cathepsin D
576 primary antibody pair, with similar results shown in Supplementary Figure 4.
577
578 We suspected that the constitutive Cathepsin D expression was coming from hemolysis
579 and vascular degeneration so that we co-stained Cathepsin D with red blood cell
580 markers (Figure 11). Cathepsin D expression in the blood vessels correlated with
581 domains of diffusive and reduced HBA staining, an indication of red cell damage

582 (Figure 11A, top panel). Cathepsin D expression also associated with HBA staining in
583 CAA and dense-core plaques, which additionally overlapped with plaque MetaBlue
584 staining (Figure 11A, bottom two panels). Another red blood cell marker HbA1C also
585 associated with Cathepsin D expression in CAA blood vessels, in diffusive MetaBlue
586 positive areas, and in dense-core senile plaques with strong MetaBlue signals (Figure
587 11B). These staining results suggested that the constitutive Cathepsin D in senile
588 plaques likely derived from hemolysis.
589
590

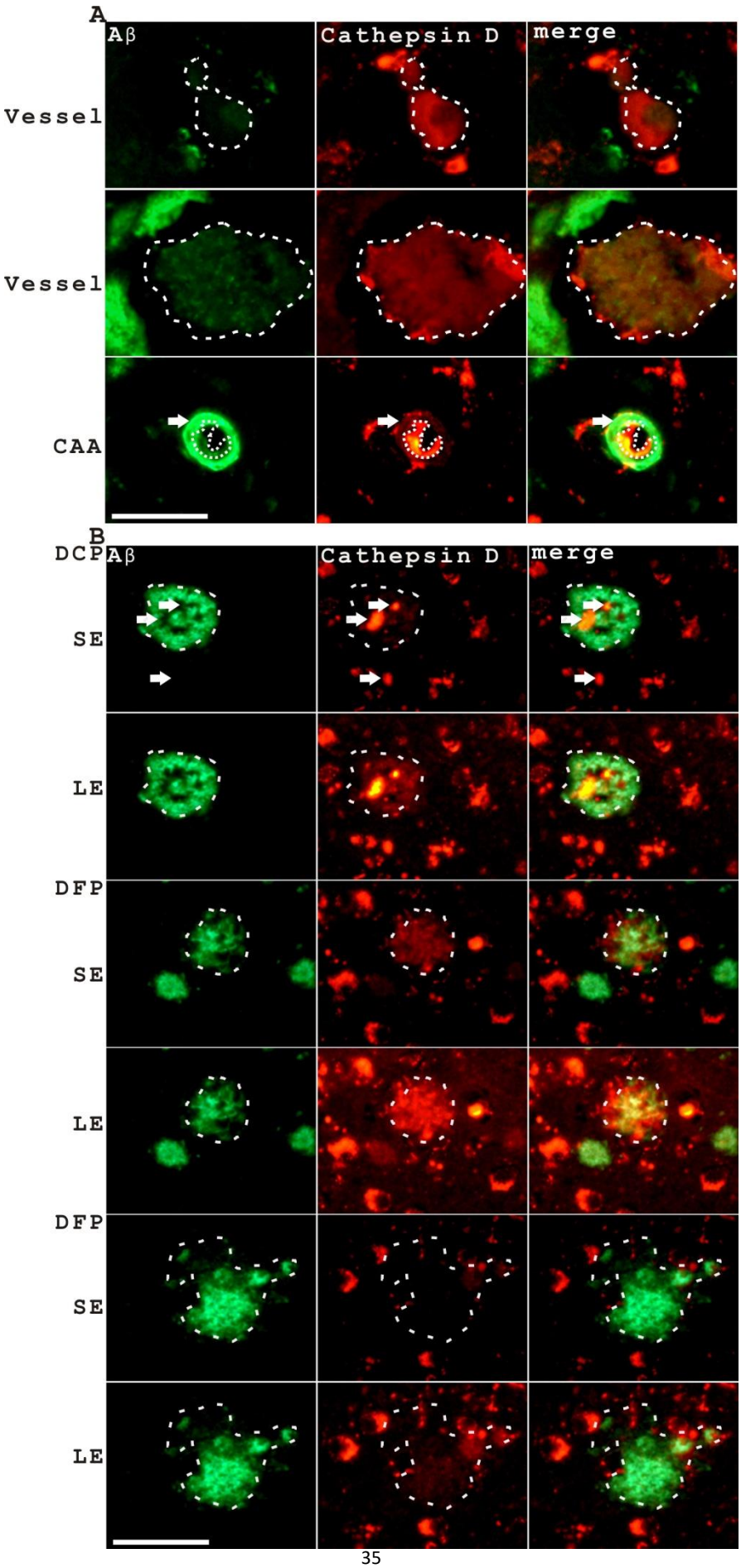
A
Aβ
Cathepsin D
merge
Vessel
Vessel
CAA
B
DCP
Aβ
Cathepsin D
merge
SE
LE
DFP
SE
LE
DFP
SE
LE

591

592 **Figure 10. The association of Aβ and Cathepsin D in blood vessels and in senile**
593 **plaques. A.** Diffusive Aβ staining associated with diffusive Cathepsin D staining in the
594 blood vessels. Diffusive Aβ staining co-distributed with diffusive Cathepsin D staining
595 in non-CAA type of blood vessel lumen (top two panels). Aβ staining also associated
596 with Cathepsin D staining in the lumen of a CAA blood vessel (bottom panel).
597 Cathepsin D staining on the CAA vessel wall was also observed. Dashed lines indicated
598 vessel diffusive Cathepsin D and Aβ staining. The arrow indicated a CAA blood vessel.
599 **B.** Senile plaques overlapped with a constitutive but relatively weak Cathepsin D
600 expression. A dense-core senile plaque (top two panels, DCP) had two distinct pattern
601 of Cathepsin D staining. A strong and granule-like Cathepsin D staining showed at
602 complementary positions relative to Aβ staining with the Cathepsin D image taken at a
603 short exposure of 0.5 second (SE stands for short exposure) while the exposure setting
604 for Aβ staining was not changed. A weaker and diffusive Cathepsin D staining co-
605 distributed with Aβ staining in the senile plaques was also observed with the Cathepsin
606 D image taken at a longer exposure of 1 second (LE stands for long exposure). The
607 exposure setting of Aβ images was unchanged. A diffusive plaque (middle two panels,
608 DFP) also showed a constitutive Cathepsin D staining that co-distributed with Aβ
609 staining but not totally matching the outline of the senile plaque. A large diffusive
610 plaque (bottom two panels, DFP) with less detectable constitutive Cathepsin D staining.
611 Dashed lines indicated the regions of senile plaques. The arrows indicated strong and
612 granule-like Cathepsin D staining. Scale bar, 50 μm.
613
614

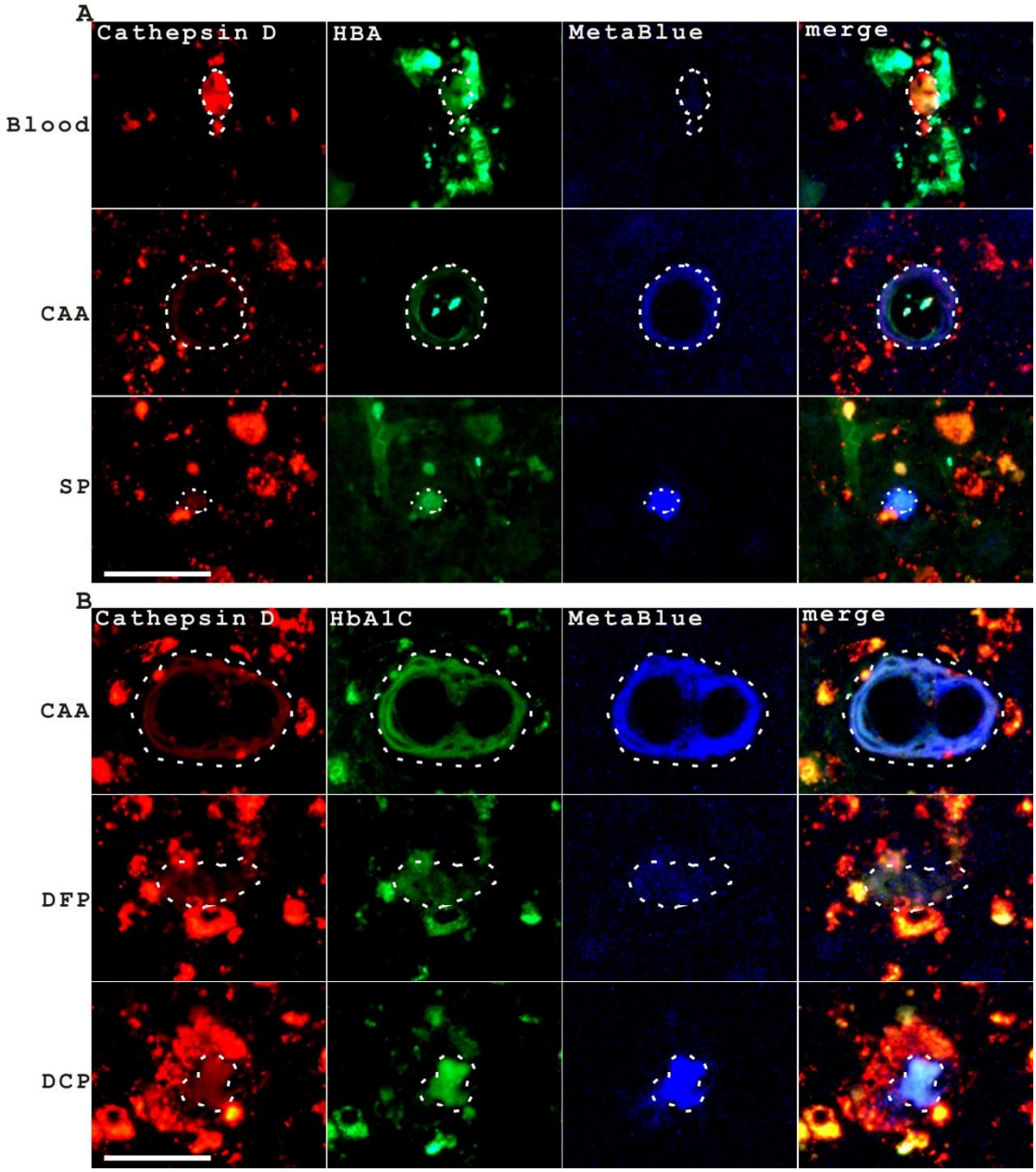

Figure 11. The association of Cathepsin D and hemoglobin in CAA and in senile plaques. A. Cathepsin D staining associated with HBA staining in the blood vessels, CAA and senile plaques. Cathepsin D staining associated with reduced RBC HBA staining (indicated with dashed lines in the top panel). Cathepsin D staining also associated with HBA staining in a CAA blood vessel with concurrent MetaBlue staining (indicated with dashed lines in the middle panel). In the bottom panel, a senile plaque (SP) (marked with dashed lines) showed both Cathepsin D and HBA staining with also a strong MetaBlue staining. **B.** Cathepsin D staining associated with HbA1c staining in

625 CAA, diffusive patches and senile plaques. Cathepsin D staining associated with
626 HbA1C staining in a CAA blood vessel (top panel). A region of diffusive Cathepsin D
627 staining also co-expressed diffusive HbA1C staining and MetaBlue staining was shown
628 in the middle panel. A dense-core senile plaque structure with both Cathepsin D and
629 HbA1C staining and also strong MetaBlue signals were shown at the bottom panel.
630 Dashed lines indicated the selected regions of Cathepsin D and HbA1C co-expression.
631 Scale bar, 50 μm.
632
633 **The specific association of Cathepsin D and ApoE with Aβ in hemolysis in AD**
634 **brain tissues.**
635
636 Since accumulating evidence pointed out the importance of hemolysis during senile
637 plaque formation, we did a more focused experiment investigating hemolysis in AD
638 tissues. In a previous investigation regarding the relation between copper ions and
639 senile plaque formation, we unexpectedly found that a copper iron staining dye named
640 Rhodanine could be a good histological staining reagent of red blood cells and
641 hemolysis as shown in Figure 12. Using this dye, we observed that there was
642 widespread intravascular hemolysis or extravascular hemolysis in AD tissues. This dye
643 also labels CAA blood vessels, confirming the relation between CAA and hemolysis
644 (Figure 12A). Rhodanine staining associated with the whole spectrum of Aβ staining
645 patterns related to senile plaque formation, from initially very weak expression in
646 phenotypically normal red blood cells to enhanced Aβ staining in hemolysis, to strong
647 staining in CAA and senile plaques (Figure 12B). In diffusive senile plaques,
648 Rhodanine staining was very weak, suggesting that Rhodanine-positive substances
649 might be metabolized after hemolysis during the course of senile plaque development
650 (Figure 12B, bottom).
651
652 With Rhodanine staining as a tool to detect hemolysis, we analyzed the interaction
653 between Aβ with Cathepsin D or ApoE during hemolytic events (Figure 13). The
654 experiment results indicated a tight coupling of the Cathepsin D-Aβ association or

ApoE-Aβ association with hemolysis, regardless the hemolysis happened intravascularly or extravascularly. Aβ staining in hemolysis was usually weaker than mature senile plaques (Figure 13A, top two panels and Figure 13B, top two panels). However, we frequently observed some strongly-stained Aβ aggregates began to form from the weakly-stained Aβ-positive hemolytic areas with overlapping Cathepsin D or ApoE staining (Figure 13A, bottom panel and Figure 13B, bottom panel). These results suggested that hemolytic domains might be the initial seeding and fermenting grounds of amyloid aggregate formation. To our knowledge, this is the first time that a transitional stage for senile plaque formation has been defined.

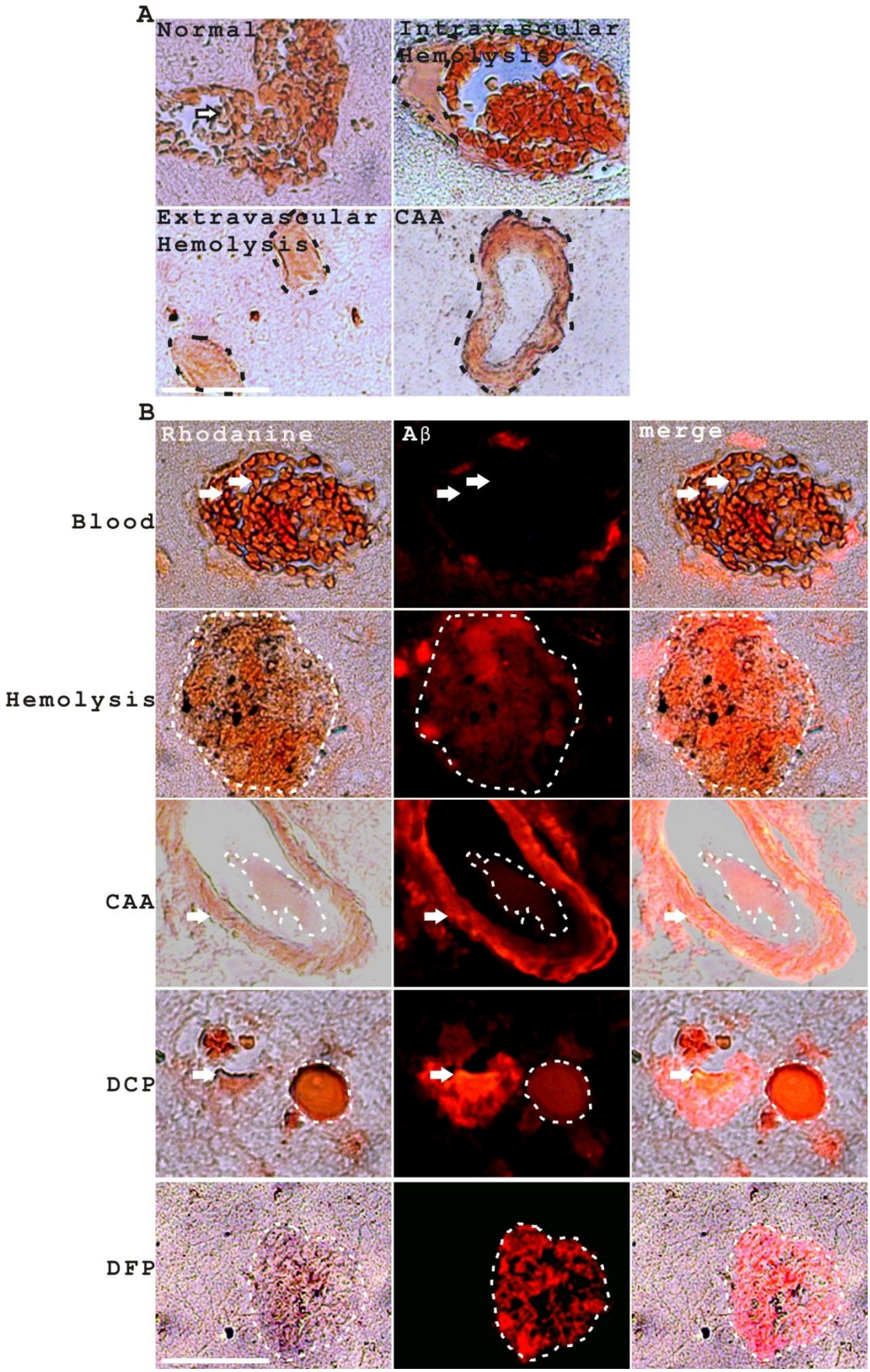
A
Normal
Intravascular Hemolysis
Extravascular Hemolysis
CAA
B
Rhodanine
Aβ
merge
Blood
Hemolysis
CAA
DCP
DFP

666

667

Figure 12. Rhodanine staining showed widespread hemolysis in AD brain tissues. **A.** Rhodanine staining was a good marker of normal red blood cells, which also stained hemolysis, and CAA in AD brain tissues. **B.** Rhodanine staining was present in normally looking red blood cells without strong Aβ staining and at all different stages of senile plaque development including hemolysis, CAA with hemolysis, dense-core plaques (DCP) and diffusive plaques (DFP) with enhanced Aβ staining. Scale bar, 50 μm.

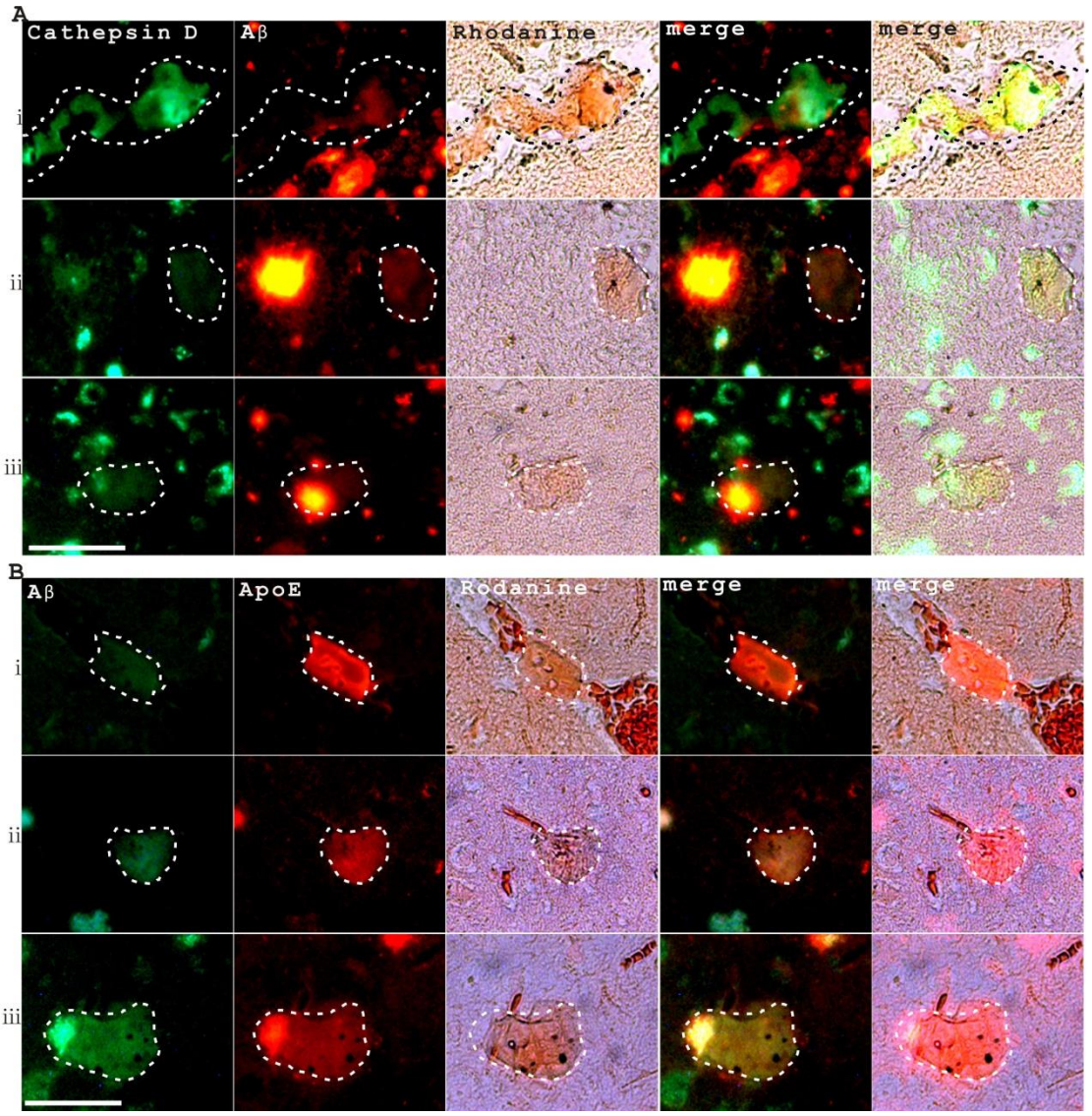

Figure 13. Cathepsin D and ApoE both associated with Aβ specifically in hemolysis. **A.** Cathepsin D associated with Aβ in intravascular hemolysis (ⅰ) and extravascular hemolysis (ⅱ, ⅲ). Some strong Aβ staining was observed in (ⅲ). **B.** ApoE associated

with Aβ specifically in intravascular hemolysis (ⅰ) and in extravascular hemolysis (ⅱ, ⅲ). Some strong Aβ staining was observed in (ⅲ). Scale bar, 50 μm.

Aβ forms protease-sensitive heterooligomer rapidly with hemoglobin while Aβ self-oligomers are protease-resistant.

Since the senile plaque formation process might start from hemolysis, we thought the initial Aβ aggregation might also have something to do with hemolysis. We hypothesized that HBA physically interacts with Aβ during hemolytic events. The potential interaction between hemoglobin and Aβ has been studied in the past in a few published studies[47,48], but the investigations were still not complete and comprehensive. We tested this hypothesis further with an aggreagation assay in the test tubes. First, we checked the self-oligomerization of Aβ peptides (Figure 14). Both Aβ40 and Aβ42 formed small aggregates immediately soon after dissolving the peptides in DMSO and diluted into PBS solution at 5 μM concerntration. Aβ40 formed aggregates with increasing size upon incubation up to 3 days, while the sizes of Aβ42 self-oligomer did not change significantly upon prolonged incubation (Figure 14A). Both Aβ 40 and Aβ42 aggregates were resistant to a 15-minute Proteinase K （PK） treatment, suggesting the self aggregates were protease-resistant (Figure 14B).

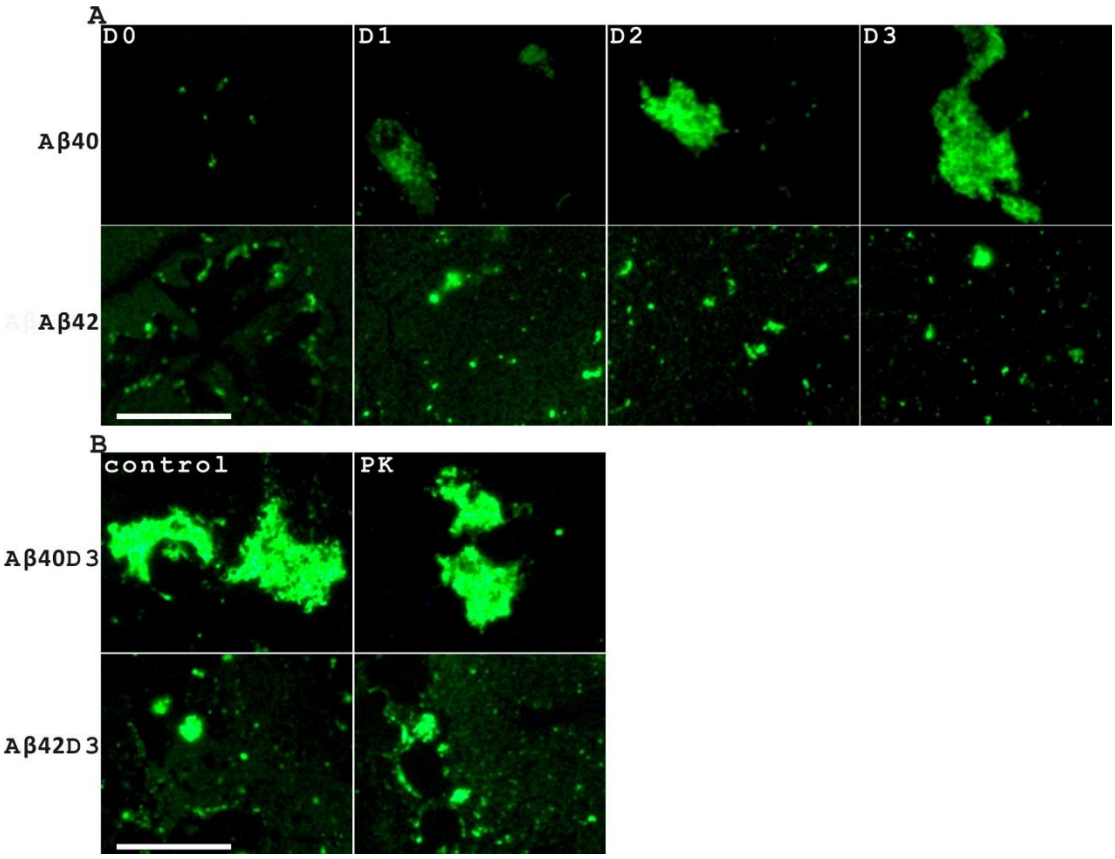

Figure 14. Aβ40 and Aβ42 form protease-resistant self-oligomers *in vitro*. A. Aβ40 and Aβ42 formed self-oligomers when incubating in PBS solution for up to 3 days (Day 0 to Day 3) followed with a drying up procedure by droplet evaporation. D0 stands for Day 0. **B.** Both Aβ40 and Aβ42 self-oligomers were resistant to Proteinase K (PK) treatment. Scale bar, 50 μm.

We then incubated hemoglobin and Aβ40 at a molar ratio of 1:4 (1.25 μM hemoglobin and 5 μM Aβ40), and checked the aggregation product out of this mixture. We observed that hemoglobin formed complexes with Aβ40 very quickly. Even in Day 0 samples, hemoglobin formed large leaf-like or ring-shape complexes with Aβ40 (Figure 15A, top two panels). Some dot-like structures dervied from Aβ40 self-oligomerization were also present in Day 0 samples (Figure 15A, third panel). Large leaf-like structures and ring-shape structures were continually present in Day 1, Day 2, Day 3 samples (Figure 15A, bottom four panels). In AD tissue samples, we did not observe large-leaf like structures with Aβ staining. However, we did observe some ring-shape structures with

718 overlapping staining of Aβ and hemoglobin (Figure 15B). This probably also explained
719 the ring-shape structures in Figure 9, which suggested that the ring-shape Aβ/Hb
720 complexes did form in the blood vessels of AD tissues *in vivo*.
721
722

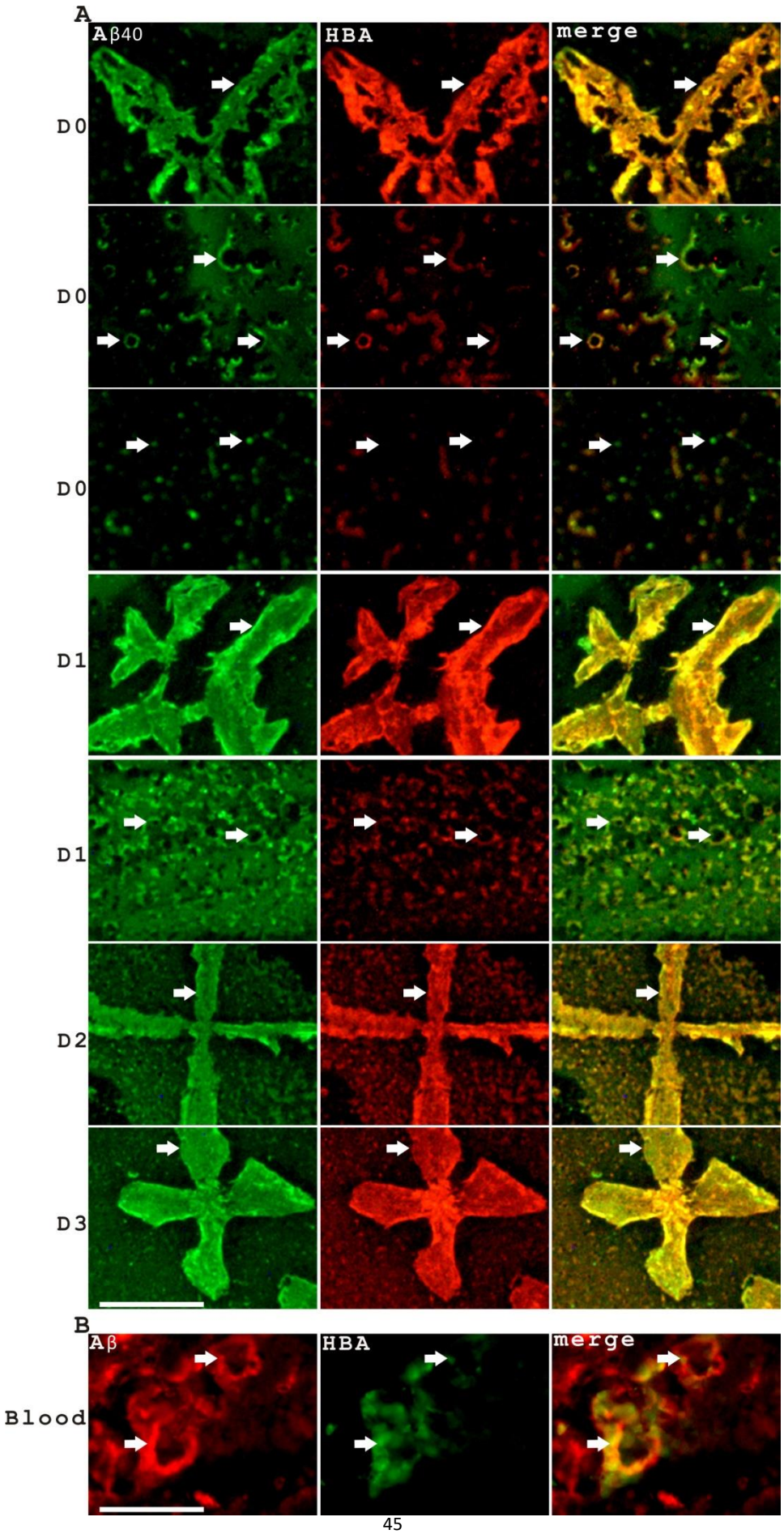

723

724 **Figure 15. Aβ40 forms heterooligomer rapidly with hemoglobin. A.** Aβ40 forms
725 heterooligomer rapidly with hemoglobin when co-incubating in PBS solution for up to
726 3 days followed with sample drying by droplet evaporation. Co-immunostaining of Aβ
727 and hemoglobin was shown for Day 0 (top 3 panels), Day 1 (fourth and fifth panels),
728 Day 2 (the sixth panel) and Day 3 (the seventh panel) samples. Arrows indicated
729 different structures, such as leaf-shape, ring-shape structures, that co-stained with both
730 Aβ and HBA (alpha hemoglobin) antibodies. The dot shape structure likely represented
731 Aβ40 self-oligomers. Special ring shape structures were indicated with arrows in the
732 second and fifth panel. **B.** Aβ40 forms ring-shape structures interacting with
733 hemoglobin in the lumens of AD patient blood vessels similar to the ring-shape
734 structures formed in Aβ and hemoglobin mixture samples *in vitro*. Scale bars, 50 μm.
735
736 In Aβ42 and Hb mixed Day 0 samples, we observed leaf-shape, ring-shape, and line-
737 shape structures with both Aβ42 and Hb staining (Figure 16). In Day 0 samples, we also
738 see the existence of Aβ42 self-oligomers, which was less frequently detected in Day 1,
739 Day 2 and Day 3 samples (Figure 16A), indicating that Aβ42/Hb interactions might
740 compete out Aβ42 self-oligomerization. Previous studies suggested that hemin inhibits
741 Aβ aggregation[49,50] and hemoglobin might interact with Aβ through the hemin motif[48],
742 suggesting that a hemoglobin inhibition of Aβ self-oligomerization is likely. Large leaf-
743 shape or smaller ring-shape structures were continually observed in Day 1, Day 2 and
744 Day 3 samples (Figure 16, bottom three panels). Unlike the protease-resistant Aβ40 and
745 Aβ42 self-oligomers, Aβ40/Hb and Aβ42/Hb hetero-complexes were both sensitive to
746 PK treatment (Figure 16B).
747
748

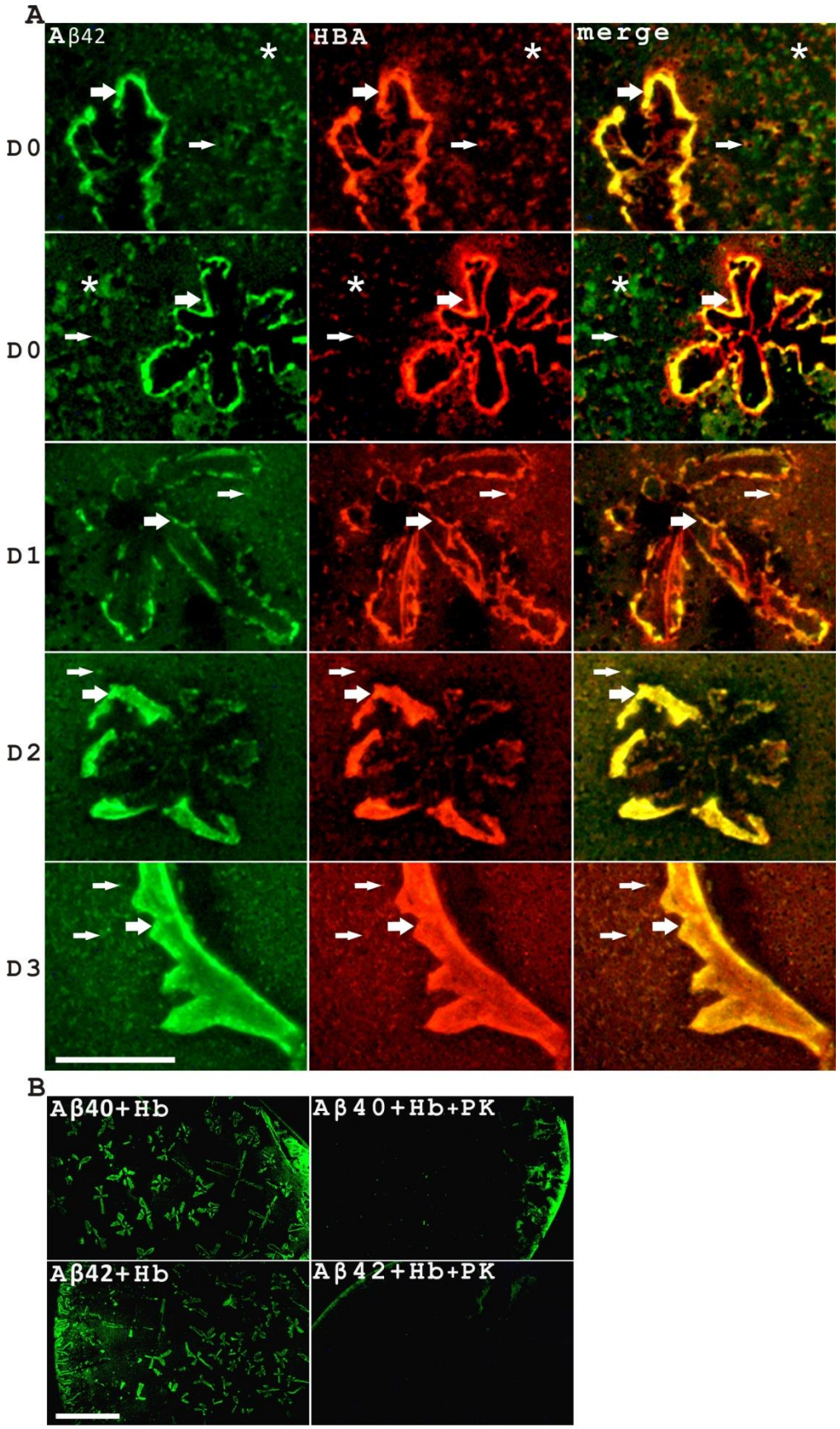

749

750

751 **Figure 16. Aβ42 forms protease-sensitive heterooligomer rapidly with hemoglobin**

752 **when co-incubating in PBS solution for up to 3 days followed with sample drying**
753 **by droplet evaporation. A.** Aβ42 forms heterooligomer rapidly with hemoglobin in
754 PBS solution. Co-immunostaining of Aβ and hemoglobin was shown for Day 0 (top
755 two panels), Day 1 (third panel), Day 2 (fourth panel) and Day 3 (fifth panel) samples.
756 Large arrows indicated relatively large structures while small arrows indicated smaller
757 structures. Leaf-shape, ring-shape or dot-shape structures were observed. Some self-
758 oligomers also existed in Day 0 samples, indicated with asterisks. Scale bar, 50 μm. **B.**
759 Both Aβ40/Hb and Aβ42/Hb complexes were protease-sensitive with the complexes
760 illustrated by Aβ antibody staining. PK treatment drastically decreased the signals of
761 resulting complexes. Scale bar, 200 μm.
762
763 **Discussion**
764
765 Senile plaque Aβ has been hypothesized to be derived from neural or vascular/blood
766 source[7,12,15,51]. This study indicated the primary direct source of Aβ is not neural cell
767 with the evidence showing a lack of substantial overlapping of senile plaque Aβ with
768 neural markers. Additionally, Aβ expression in neural cells appears to be too low to
769 account for the high density Aβ expression in senile plaques. Instead, senile plaque Aβ
770 most likely comes from red blood cell-associated Aβ leakage out of damaged blood
771 vessels. The evidence is the following: Firstly, red blood cells in AD patients were
772 clearly stained with Aβ antibody, especially in hemolytic red blood cells. Secondly,
773 strongly-stained Aβ aggregates emerged in the hemolytic regions thus hemolytic areas
774 were likely the initial seeding grounds of Aβ aggregation. Thirdly, senile plaque Aβ co-
775 distributed with multiple blood markers such as HBA, HbA1C, ApoE and red blood
776 cell-associated MetaBlue autofluorescence at multiple stages of senile plaque
777 development such as CAA, dense-core plaques and diffusive plaques.
778
779 Two important aspects of senile plaque formation are the source of Aβ peptides and the
780 source of beta-site cutting enzymes. This study indicated that hemolysis could be a
781 critical step that bring together Aβ-related peptides and Cathepsin D, a potential beta-

site cutting enzyme, which might help to initiate the Aβ aggregation process. Platelets could be an important source of Aβ-related peptides in the blood and in hemolysis. Our experiment indicated that CD42b-positive platelets are stained positive for Aβ in the blood vessel lumen and on the blood vessel walls. Since platelets can release AβPP in alpha-granules after platelet activation by hemolysis or vascular damage[26,52-54]， it is possible that some of Aβ that associated with red blood cells were actually derived from platelets. HBA, CD42b and Rhodanine staining indicated that both hemolysis and coagulation were present in AD blood vessels, suggesting that the disrupted blood homeostasis is a fundamental defect in AD patients. Cathepsin D could be released by various cell types, including platelets[55], mast cells[56], neutrophils[57], or cytotoxic lymphocytes[58] that are activated under pathological conditions such as hemolysis or coagulation. In addition, Cathepsin D could be released from the degenerated cells of the vessel wall. Along with other factors that might affect blood vessel permeability such as histamine[59], the Cathepsin D and Aβ enriched hemolytic mixture could digest the vasculature and cause enzymatic damage to the blood vessels, which induces further leakage， extracellular matrix digestion and the formation of CAA. When the blood vessel integrity is compromised with leakage or all-out degeneration, the Cathepsin D and Aβ enriched mixture with some invasive ability provided by the proteases entered the brain parenchyma, promoting the formation of senile plaques. Although Cathepsin D could be a very important protease for amyloid aggregation，given the drastic changes and multiple cell types involving hemolysis, vascular degeneration and neuronal inflammation, the participation of multiple proteases such as BACE1[34,35], Cathepsin B[39,40], Carboxypeptidase B[41] or MMP2[42] in this complicate process is possible.

Hemolysis likely also initiates many important molecular interactions in the senile plaques. This study provided both histological and biochemical evidence that Aβ might interact with hemoglobin physically. During hemolysis, with abundant Aβ and hemoglobin, Aβ/Hb ring-shape heterooligomers might be early-stage aggregates in the hemolytic regions. The interaction between Aβ and Hb could be physiologically important as previous research suggested that Aβ binding reduces hemin toxicity[48].

812 Although Aβ peptides were frequently shown to be cytotoxic to neural cells *in vitro*，
813 since Aβ/Hb complex formation can compete with Aβ self-oligomerization, the
814 possibility of senile plaques serving as Aβ peptide reservoirs to prevent Hb-related
815 toxicity in future hemorrhage events should not be excluded. Our experiment showed
816 that Aβ/Hb complex was sensitive to protease digestion but Aβ self-oligomers were
817 protease resistant, which explains why Aβ stands out as the everlasting and more stable
818 component of senile plaques. The association between ApoE and Aβ was also
819 happening during hemolysis and this association continued to be present in CAA and
820 senile plaques, indicating ApoE is also an early responder to hemolysis and an
821 important component of the senile plaque. The presence of ApoE in the senile plaques
822 has also been reported previously by other research groups[60,61]. In addition, ApoE
823 knockout mice have a strong atherosclerosis phenotype, emphasizing its importance as
824 a blood homeostasis regulator[62-64].
825
826 Previous studies in AD patients and in mouse models of AD have already found that
827 dense-core plaques are centered on vessel walls[13,14]. These studies suggested that
828 perturbed vascular transport and/or perivascular enrichment of neuronal Aβ leads to the
829 formation of vasocentric dense plaques. Our results showed that many dense-core
830 plaques are intermingled with degenerated vessel fragments by ColIV, ACTA2 and
831 LRP1 staining, providing further evidence that vascular degeneration is intrinsically
832 linked with senile plaque formation. However, we think that senile plaque Aβ is
833 primarily derived from the blood source although the additional contribution of Aβ from
834 vascular cells or neural cells is possible. A series of studies by Dr. Cullen's group using
835 thick brain tissue sections showed a clear anatomic link between microhemorrhage with
836 senile plaque formation and also Tau phosphorylation[12,17,18]. Yet，in these studies, the
837 exact source of Aβ was still not clear. With Rhodanine staining instead of Perls staining,
838 our study provided a direct link between blood Aβ expression and hemolysis,
839 suggesting that damaged red blood cells were enriched for Aβ. We also established a
840 link between enhanced Aβ staining with vascular damage, which is not surprising since
841 blood cell abnormality is frequently linked with vascular damage. In addition, we

842 provided biochemical evidence that hemoglobin might form complexes directly with
843 Aβ. In summary, our data suggested that the senile plaque formation is primarily
844 induced by the leakage of hemolytic red blood cells along with other blood contents
845 with CAA and vascular degeneration as intermediate steps. Although amyloid cascade
846 hypothesis is an attractive and straightforward hypothesis as it stands, however, the
847 mechanism of Alzheimer's disease might be much more complicated than previously
848 thought. The AD research field should pay careful attention to the accumulating
849 substantial evidence showing the linkage between senile plaque formation and vascular
850 degeneration and blood abnormalities such as microhemorrhage and hemolysis and be
851 open-minded about revisions on current concepts.
852
853 The findings that senile plaques are associated with specific blue autofluorescence are
854 intriguing. There have been a number of studies related to senile plaque blue
855 autofluorescence materials (temporarily named as MetaBlue in this article) in the
856 past[22,23,65]. An early study reported that the blue autofluorescence was associated with
857 senile plaques but not CAA[22]. Two more recent studies found that the blue
858 autofluorescence was associated with both senile plaques and CAA[23,65]. Our study
859 additionally found that MetaBlue was not only associated with CAA and senile plaques
860 but also directly associated with red blood cells. The existence of MetaBlue
861 fluorescence in different kind of senile plaques with different sizes suggests that
862 MetaBlue could be an important component of senile plaques. The exact identity of
863 MetaBlue is unknown. MetaBlue could be an oxidative-stress related metabolite since
864 previous literature indicated that the blue autofluorescence of amyloid peptides could
865 be associated with tyrosine oxidation[66]. To isolate MetaBlue materials and to elucidate
866 the true identity of MetaBlue will likely leads to deeper understanding of AD
867 pathogenesis.
868
869 **Data and materials availability.** All data needed to evaluate the conclusions in this
870 paper are present either in the main text or in the supplementary materials.
871

Supplementary Materials.

Supplementary Figures 1-4

Acknowledgements: We want to thank the great help from Dr. Ma Chao and Dr. Qiu Wenying for providing AD tissue sections from National Human Brain Bank for Development and Function, Chinese Academy of Medical Sciences and Peking Union Medical College, Beijing, China. Additionally, we want to thank Dr. Xiangli Zhang of Shandong University for valuable discussions. We also want to thank Shunjie Wu from Keyence Co. for allowing us to use their Keyence BZ-X800 microscope without charge. Furthermore, we want to thank Housheng Wang, Lu Xu, Wenting Xuan, Pingxin Liu, Xiaoyi Bao, and Jun Wang for excellent lab assistance. **Funding**: This work was supported by National Natural Science Foundation of China No. 81472235 (H.F.), Shanghai Jiao Tong University Research Grant YG2017MS71 (D.P. and H.F.). **Author contributions:** H.F. conceived the study; H. F. designed and supervised the experiments; H.F. and J. L. performed the experiments; H. F., J. L., D.P., W. J., G. G., D. C. did the data analysis; H. F. wrote the manuscript; All authors reviewed the manuscript. **Competing interests:** Authors declare no competing interests.

References:

1 Lane, C. A., Hardy, J. & Schott, J. M. Alzheimer's disease. *Eur J Neurol* **25**, 59-70, doi:10.1111/ene.13439 (2018).

2 Attems, J., Lintner, F. & Jellinger, K. A. Amyloid beta peptide 1-42 highly correlates with capillary cerebral amyloid angiopathy and Alzheimer disease pathology. *Acta neuropathologica* **107**, 283-291, doi:10.1007/s00401-004-0822-6 (2004).

3 van Helmond, Z., Miners, J. S., Kehoe, P. G. & Love, S. Oligomeric Abeta in Alzheimer's disease: relationship to plaque and tangle pathology, APOE genotype and cerebral amyloid angiopathy. *Brain Pathol* **20**, 468-480, doi:10.1111/j.1750-3639.2009.00321.x (2010).

4 Glenner, G. G., Henry, J. H. & Fujihara, S. Congophilic angiopathy in the pathogenesis of Alzheimer's degeneration. *Annales de pathologie* **1**, 120-129 (1981).

5 Glenner, G. G. & Wong, C. W. Alzheimer's disease: initial report of the purification and characterization of a novel cerebrovascular amyloid protein. *Biochemical and biophysical research communications* **120**, 885-890, doi:10.1016/s0006-291x(84)80190-4 (1984).

6 Masters, C. L. *et al.* Amyloid plaque core protein in Alzheimer disease and Down syndrome.

Proceedings of the National Academy of Sciences of the United States of America **82**, 4245-4249, doi:10.1073/pnas.82.12.4245 (1985).

7 Hardy, J. A. & Higgins, G. A. Alzheimer's disease: the amyloid cascade hypothesis. *Science* **256**, 184-185, doi:10.1126/science.1566067 (1992).

8 Hardy, J. Alzheimer's disease: the amyloid cascade hypothesis: an update and reappraisal. *Journal of Alzheimer's disease : JAD* **9**, 151-153, doi:10.3233/jad-2006-9s317 (2006).

9 Miyakawa, T., Shimoji, A., Kuramoto, R. & Higuchi, Y. The relationship between senile plaques and cerebral blood vessels in Alzheimer's disease and senile dementia. Morphological mechanism of senile plaque production. *Virchows Archiv. B, Cell pathology including molecular pathology* **40**, 121-129, doi:10.1007/bf02932857 (1982).

10 Kawai, M., Kalaria, R. N., Harik, S. I. & Perry, G. The relationship of amyloid plaques to cerebral capillaries in Alzheimer's disease. *The American journal of pathology* **137**, 1435-1446 (1990).

11 Sparks, D. L., Kuo, Y. M., Roher, A., Martin, T. & Lukas, R. J. Alterations of Alzheimer's disease in the cholesterol-fed rabbit, including vascular inflammation. Preliminary observations. *Annals of the New York Academy of Sciences* **903**, 335-344, doi:10.1111/j.1749-6632.2000.tb06384.x (2000).

12 Cullen, K. M., Kocsi, Z. & Stone, J. Microvascular pathology in the aging human brain: Evidence that senile plaques are sites of microhaemorrhages. *Neurobiol Aging* **27**, 1786-1796, doi:10.1016/j.neurobiolaging.2005.10.016 (2006).

13 Kumar-Singh, S. *et al.* Dense-core senile plaques in the Flemish variant of Alzheimer's disease are vasocentric. *The American journal of pathology* **161**, 507-520, doi:10.1016/S0002-9440(10)64207-1 (2002).

14 Kumar-Singh, S. *et al.* Dense-core plaques in Tg2576 and PSAPP mouse models of Alzheimer's disease are centered on vessel walls. *The American journal of pathology* **167**, 527-543, doi:10.1016/S0002-9440(10)62995-1 (2005).

15 Bu, X. L. *et al.* Blood-derived amyloid-beta protein induces Alzheimer's disease pathologies. *Molecular psychiatry* **23**, 1948-1956, doi:10.1038/mp.2017.204 (2018).

16 Ryu, J. K. & McLarnon, J. G. A leaky blood-brain barrier, fibrinogen infiltration and microglial reactivity in inflamed Alzheimer's disease brain. *Journal of cellular and molecular medicine* **13**, 2911-2925, doi:10.1111/j.1582-4934.2008.00434.x (2009).

17 Cullen, K. M., Kócsi, Z. & Stone, J. Pericapillary Haem-Rich Deposits: Evidence for Microhaemorrhages in Aging Human Cerebral Cortex. *Journal of Cerebral Blood Flow & Metabolism* **25**, 1656-1667, doi:10.1038/sj.jcbfm.9600155 (2005).

18 Hansra, G. K. *et al.* The neuritic plaque in Alzheimer's disease: perivascular degeneration of neuronal processes. *Neurobiol Aging* **82**, 88-101, doi:https://doi.org/10.1016/j.neurobiolaging.2019.06.009 (2019).

19 Sun, H. L. *et al.* Blood cell-produced amyloid-beta induces cerebral Alzheimer-type pathologies and behavioral deficits. *Mol Psychiatr*, doi:10.1038/s41380-020-0842-1 (2020).

20 Fu, H. *et al.* Persisting and Increasing Neutrophil Infiltration Associates with Gastric Carcinogenesis and E-cadherin Downregulation. *Scientific reports* **6**, 29762, doi:10.1038/srep29762 (2016).

21 Wallin, C., Luo, J. H., Jarvet, J., Warmlander, S. K. T. S. & Graslund, A. The Amyloid-beta Peptide in Amyloid Formation Processes: Interactions with Blood Proteins and Naturally Occurring Metal Ions. *Isr J Chem* **57**, 674-685, doi:10.1002/ijch.201600105 (2017).

950 22 Dowson, J. H. A sensitive method for the demonstration of senile plaques in the dementing
951 brain. *Histopathology* **5**, 305-310, doi:10.1111/j.1365-2559.1981.tb01789.x (1981).
952 23 Gao, Y. *et al.* Imaging and Spectral Characteristics of Amyloid Plaque Autofluorescence in Brain
953 Slices from the APP/PS1 Mouse Model of Alzheimer's Disease. *Neuroscience bulletin* **35**, 1126-
954 1137, doi:10.1007/s12264-019-00393-6 (2019).
955 24 Cohen, R. M. *et al.* Red cell life span heterogeneity in hematologically normal people is
956 sufficient to alter HbA1c. *Blood* **112**, 4284-4291, doi:10.1182/blood-2008-04-154112 (2008).
957 25 Holtzman, D. M. Role of apoE/A beta interactions in the pathogenesis of Alzheimer's disease
958 and cerebral amyloid angiopathy. *J. Mol. Neurosci.* **17**, 147-155, doi:10.1385/jmn:17:2:147
959 (2001).
960 26 Li, Q. X. *et al.* Membrane-associated forms of the beta A4 amyloid protein precursor of
961 Alzheimer's disease in human platelet and brain: surface expression on the activated human
962 platelet. *Blood* **84**, 133-142 (1994).
963 27 Koupenova, M., Kehrel, B. E., Corkrey, H. A. & Freedman, J. E. Thrombosis and platelets: an
964 update. *European heart journal* **38**, 785-791, doi:10.1093/eurheartj/ehw550 (2017).
965 28 Ferguson, D. J. Acute intravascular hemolysis after a platelet transfusion. *CMAJ : Canadian*
966 *Medical Association journal = journal de l'Association medicale canadienne* **138**, 523-524
967 (1988).
968 29 Weinstein, L. Syndrome of hemolysis, elevated liver enzymes, and low platelet count: A severe
969 consequence of hypertension in pregnancy. *Am J Obstet Gynecol* **193**, 859-860,
970 doi:10.1016/j.ajog.2005.02.113 (2005).
971 30 Helms, C. C. *et al.* Mechanisms of hemolysis-associated platelet activation. *Journal of*
972 *Thrombosis and Haemostasis* **11**, 2148-2154, doi:10.1111/jth.12422 (2013).
973 31 Scheibel, A. B. Alterations of the cerebral capillary bed in the senile dementia of Alzheimer. *The*
974 *Italian Journal of Neurological Sciences* **8**, 457-463, doi:10.1007/bf02334602 (1987).
975 32 Bu, G., Cam, J. & Zerbinatti, C. LRP in amyloid-beta production and metabolism. *Ann N Y Acad*
976 *Sci*, 005 (2006).
977 33 Storck, S. E. *et al.* Endothelial LRP1 transports amyloid-beta(1-42) across the blood-brain barrier.
978 *J. Clin. Invest.* **126**, 123-136, doi:10.1172/jci81108 (2016).
979 34 Yan, R. *et al.* Membrane-anchored aspartyl protease with Alzheimer's disease β-secretase
980 activity. *Nature* **402**, 533-537, doi:10.1038/990107 (1999).
981 35 Cai, H. *et al.* BACE1 is the major β-secretase for generation of Aβ peptides by neurons. *Nature*
982 *Neuroscience* **4**, 233-234, doi:10.1038/85064 (2001).
983 36 Chevallier, N. *et al.* Cathepsin D displays in vitro beta-secretase-like specificity. *Brain Res.* **750**,
984 11-19, doi:10.1016/s0006-8993(96)01330-3 (1997).
985 37 Schechter, I. & Ziv, E. Kinetic properties of cathepsin D and BACE 1 indicate the need to search
986 for additional beta-secretase candidate(s). *Biol. Chem.* **389**, 313-320, doi:10.1515/bc.2008.025
987 (2008).
988 38 Evin, G. *et al.* Candidate gamma-secretases in the generation of the carboxyl terminus of the
989 Alzheimer's disease beta-A4 amyloid: Possible involvement of cathepsin D. *Biochemistry* **34**,
990 14185-14192, doi:10.1021/bi00043a024 (1995).
991 39 Schechter, I. & Ziv, E. Cathepsins S, B and L with aminopeptidases display β-secretase activity
992 associated with the pathogenesis of Alzheimer's disease. **392**, 555-569,
993 doi:doi:10.1515/bc.2011.054 (2011).

40 Hook, V. Y. H., Kindy, M., Reinheckel, T., Peters, C. & Hook, G. Genetic cathepsin B deficiency reduces beta-amyloid in transgenic mice expressing human wild-type amyloid precursor protein. *Biochem. Biophys. Res. Commun.* **386**, 284-288, doi:10.1016/j.bbrc.2009.05.131 (2009).

41 Matsumoto, A., Itoh, K. & Matsumoto, R. A novel carboxypeptidase B that processes native beta-amyloid precursor protein is present in human hippocampus. *Eur. J. Neurosci.* **12**, 227-238, doi:10.1046/j.1460-9568.2000.00908.x (2000).

42 Lepage, R. N. *et al.* Gelatinase A possesses a beta-secretase-like activity in cleaving the amyloid protein precursor of Alzheimer's disease. *FEBS Letters* **377**, 267-270, doi:10.1016/0014-5793(95)01358-x (1995).

43 Papassotiropoulos, A. *et al.* Genetic polymorphism of cathepsin D is strongly associated with the risk for developing sporadic Alzheimer's disease. *Neuroscience Letters* **262**, 171-174, doi:https://doi.org/10.1016/S0304-3940(99)00071-3 (1999).

44 Schuur, M. *et al.* Cathepsin D gene and the risk of Alzheimer's disease: A population-based study and meta-analysis. *Neurobiology of Aging* **32**, 1607-1614, doi:https://doi.org/10.1016/j.neurobiolaging.2009.10.011 (2011).

45 Bernstein, H. G., Bruszis, S., Schmidt, D., Wiederanders, B. & Dorn, A. Immunodetection of cathepsin D in neuritic plaques found in brains of patients with dementia of Alzheimer type. *Journal fur Hirnforschung* **30**, 613-618 (1989).

46 Cataldo, A. M., Barnett, J. L., Mann, D. M. A. & Nixon, R. A. Colocalization of Lysosomal Hydrolase and β-Amyloid in Diffuse Plaques of the Cerebellum and Striatum in Alzheimer's Disease and Down's Syndrome. *Journal of Neuropathology & Experimental Neurology* **55**, 704-715, doi:10.1097/00005072-199606000-00004 (1996).

47 Wu, C. W. *et al.* Hemoglobin promotes Abeta oligomer formation and localizes in neurons and amyloid deposits. *Neurobiology of disease* **17**, 367-377, doi:10.1016/j.nbd.2004.08.014 (2004).

48 Chuang, J. Y. *et al.* Interactions between amyloid-beta and hemoglobin: implications for amyloid plaque formation in Alzheimer's disease. *PloS one* **7**, e33120, doi:10.1371/journal.pone.0033120 (2012).

49 Howlett, D., Cutler, P., Heales, S. & Camilleri, P. Hemin and related porphyrins inhibit beta-amyloid aggregation. *FEBS letters* **417**, 249-251 (1997).

50 Liu, Y. *et al.* Hemin as a generic and potent protein misfolding inhibitor. *Biochemical and biophysical research communications* **454**, 295-300, doi:10.1016/j.bbrc.2014.10.062 (2014).

51 de la Torre, J. C. & Aliev, G. Alzheimer's disease is a vascular disorder with neurodegenerative consequences. *J Neurol Sci* **229**, 305-306 (2005).

52 Smith, R. P. & Broze, G. J., Jr. Characterization of platelet-releasable forms of beta-amyloid precursor proteins: the effect of thrombin. *Blood* **80**, 2252-2260 (1992).

53 Van Nostrand, W. E., Schmaier, A. H., Farrow, J. S. & Cunningham, D. D. Platelet protease nexin-2/amyloid beta-protein precursor. Possible pathologic and physiologic functions. *Annals of the New York Academy of Sciences* **640**, 140-144, doi:10.1111/j.1749-6632.1991.tb00205.x (1991).

54 Canobbio, I. *et al.* Platelet amyloid precursor protein is a modulator of venous thromboembolism in mice. *Blood* **130**, 527-536, doi:10.1182/blood-2017-01-764910 (2017).

55 Rendu, F. & Brohard-Bohn, B. The platelet release reaction: granules' constituents, secretion and functions. *Platelets* **12**, 261-273, doi:10.1080/09537100120068170 (2001).

56 Puri, N. & Roche, P. A. Mast cells possess distinct secretory granule subsets whose exocytosis

1038 is regulated by different SNARE isoforms. *Proc Natl Acad Sci U S A* **105**, 2580-2585 (2008).
1039 57 Conus, S. *et al.* Caspase-8 is activated by cathepsin D initiating neutrophil apoptosis during the
1040 resolution of inflammation. *J Exp Med* **205**, 685-698 (2008).
1041 58 Burkhardt, J. K., Hester, S., Lapham, C. K. & Argon, Y. The lytic granules of natural killer cells are
1042 dual-function organelles combining secretory and pre-lysosomal compartments. *The Journal*
1043 *of cell biology* **111**, 2327-2340, doi:10.1083/jcb.111.6.2327 (1990).
1044 59 Sedeyn, J. C. *et al.* Histamine Induces Alzheimer's Disease-Like Blood Brain Barrier Breach and
1045 Local Cellular Responses in Mouse Brain Organotypic Cultures. *Biomed Res Int* **937148**, 30
1046 (2015).
1047 60 Namba, Y., Tomonaga, M., Kawasaki, H., Otomo, E. & Ikeda, K. Apolipoprotein E
1048 immunoreactivity in cerebral amyloid deposits and neurofibrillary tangles in Alzheimer's
1049 disease and kuru plaque amyloid in Creutzfeldt-Jakob disease. *Brain Res.* **541**, 163-166,
1050 doi:https://doi.org/10.1016/0006-8993(91)91092-F (1991).
1051 61 Wisniewski, T. & Frangione, B. Apolipoprotein E: A pathological chaperone protein in patients
1052 with cerebral and systemic amyloid. *Neuroscience Letters* **135**, 235-238,
1053 doi:https://doi.org/10.1016/0304-3940(92)90444-C (1992).
1054 62 Nakashima, Y., Plump, A. S., Raines, E. W., Breslow, J. L. & Ross, R. ApoE-deficient mice develop
1055 lesions of all phases of atherosclerosis throughout the arterial tree. *Arteriosclerosis and*
1056 *Thrombosis* **14**, 133-140, doi:10.1161/01.atv.14.1.133 (1994).
1057 63 Seo, H. S. *et al.* Peripheral vascular stenosis in apolipoprotein E-deficient mice. Potential roles
1058 of lipid deposition, medial atrophy, and adventitial inflammation. *Arterioscler Thromb Vasc Biol*
1059 **17**, 3593-3601 (1997).
1060 64 Rosenfeld, M. E. *et al.* Advanced atherosclerotic lesions in the innominate artery of the ApoE
1061 knockout mouse. *Arterioscler Thromb Vasc Biol* **20**, 2587-2592 (2000).
1062 65 Kwan, A. C., Duff, K., Gouras, G. K. & Webb, W. W. Optical visualization of Alzheimer's pathology
1063 via multiphoton-excited intrinsic fluorescence and second harmonic generation. *Opt Express*
1064 **17**, 3679-3689, doi:10.1364/Oe.17.003679 (2009).
1065 66 Fricano, A., Librizzi, F., Rao, E., Alfano, C. & Vetri, V. Blue autofluorescence in protein aggregates
1066 "lighted on" by UV induced oxidation. *Biochimica et biophysica acta. Proteins and proteomics*
1067 **1867**, 140258, doi:10.1016/j.bbapap.2019.07.011 (2019).
1068
1069
1070
1071

1072 # Supplementary Information for

1073

1074 **Senile plaques arise from Cathepsin D and Aβ-enriched**

1075 **proteinaceous mixtures out of hemolysis and vascular degeneration**

1076 Hualin Fu, Jilong Li, Peng Du, Weilin Jin, Guo Gao, Daxiang Cui

1077

1078 **This PDF file includes:**

1079

1080 Supplementary Fig. 1 to 4

1081

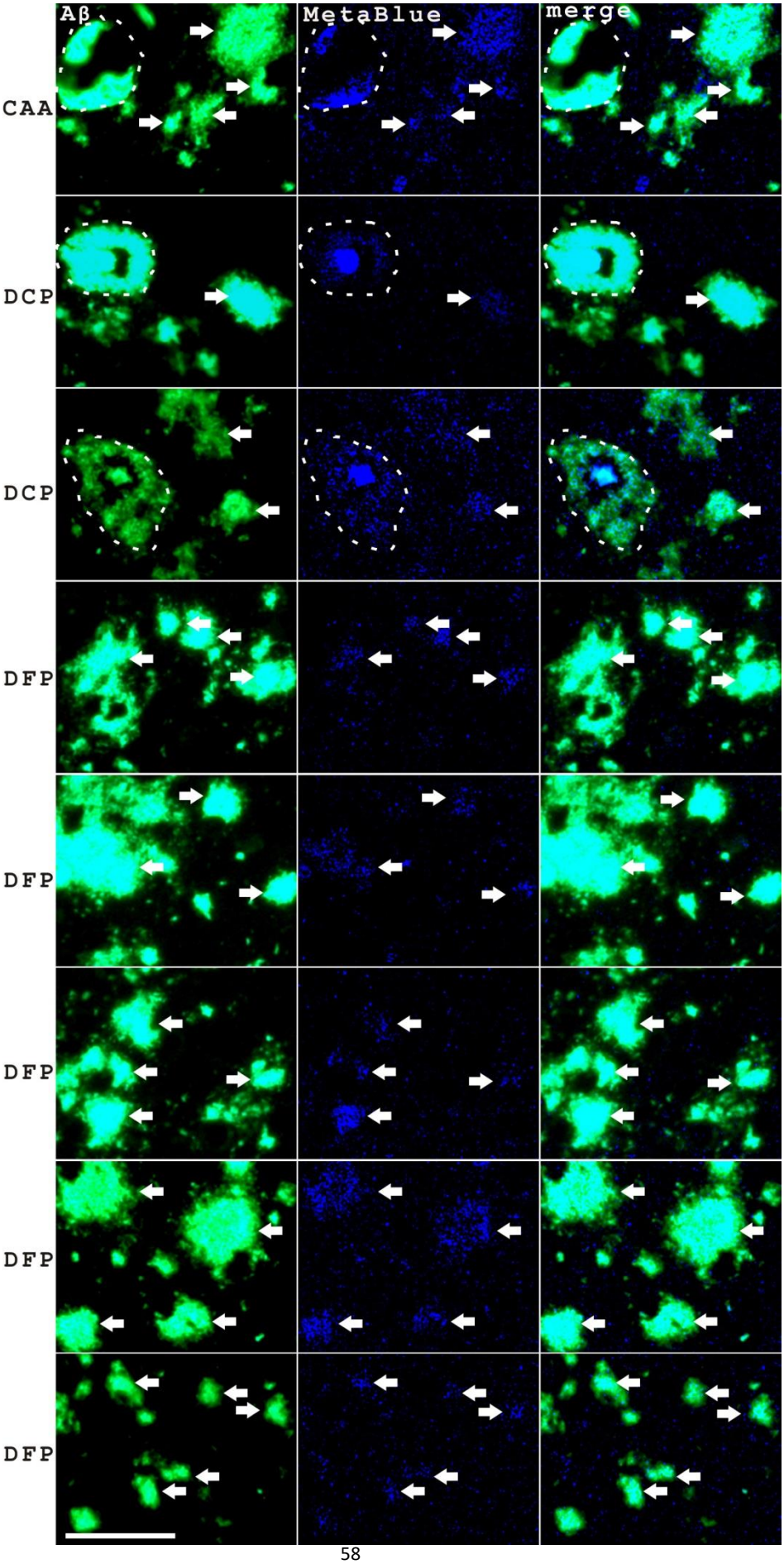

1082

1083 **Supplementary Figure 1. MetaBlue is a robust and consistent marker of senile**
1084 **plaques.** MetaBlue and Aβ staining in CAA (top panel), dense-core plaques (second
1085 and third panels, DCP) and in diffusive plaques (bottom five panels, DFP) was shown
1086 in this figure. Dashed lines indicated CAA or dense-core plaques while the arrows
1087 indicated diffusive plaques. Scale bar, 50 μm.
1088

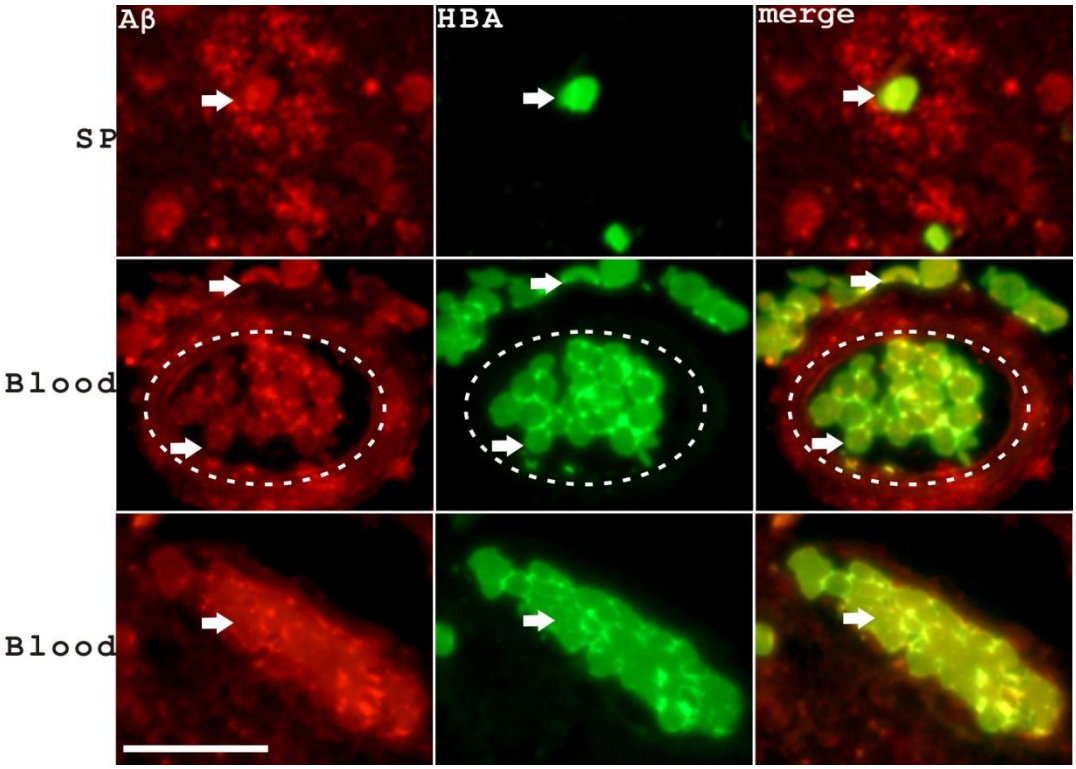

1089
1090 **Supplementary Figure 2. The co-expression of Aβ and red blood cell marker alpha**
1091 **hemoglobin (HBA).** Aβ staining of a single red blood cell marked with HBA in the
1092 center of a senile plaque was shown in the top panel. Aβ staining of red blood cells
1093 marked with HBA during red blood cell extravasation was shown in the middle panel.
1094 Aβ staining of red blood cells marked with HBA during intravascular hemolysis with
1095 the disappearance of clear round shape structure of red blood cells was shown at the
1096 bottom. The arrow indicated Aβ and HBA co-staining. The dashed lines indicated the
1097 outline of a blood vessel. Scale bar, 50 μm.
1098

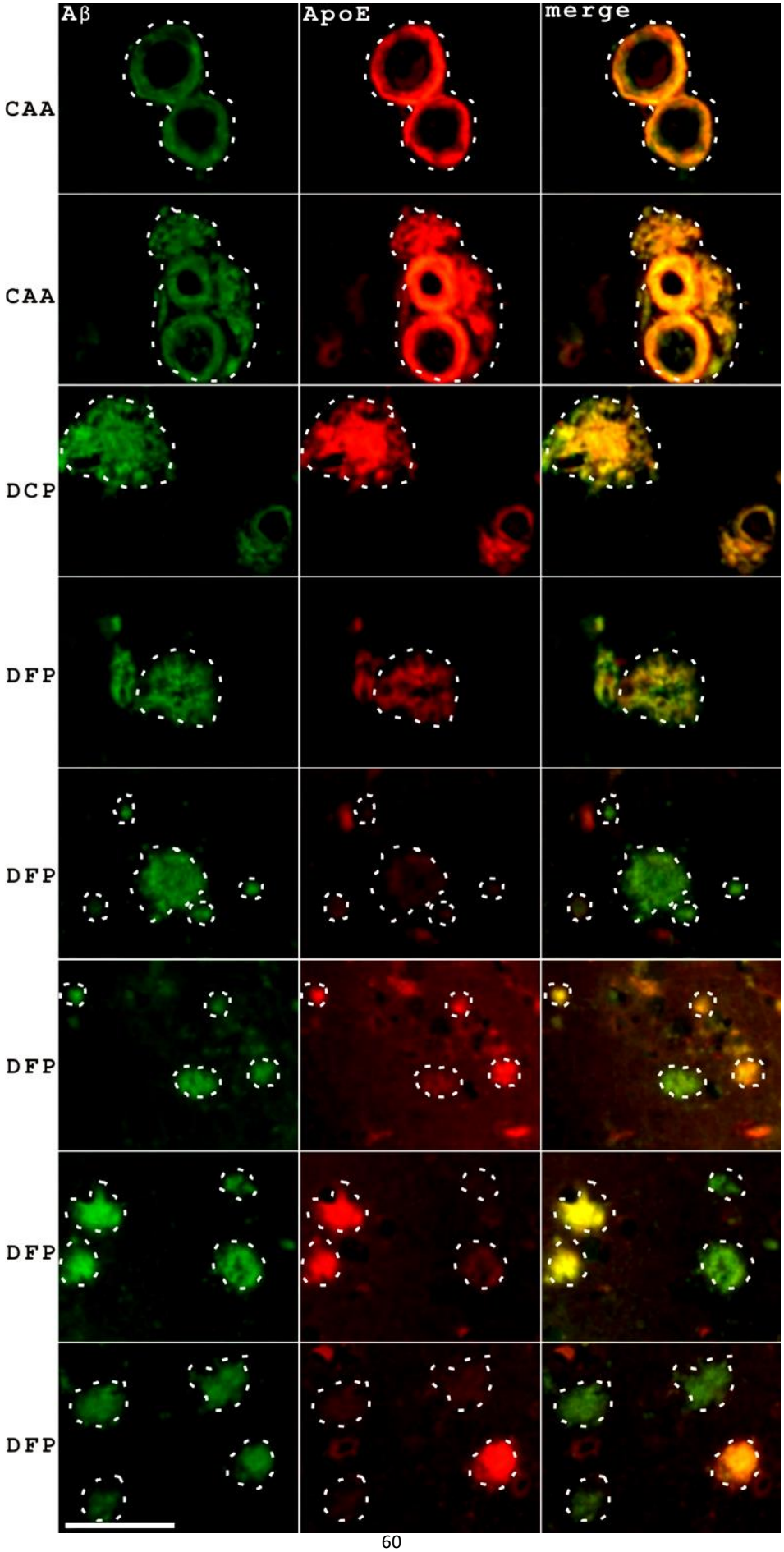

1099

1100 **Supplementary Figure 3. ApoE is a constitutive component of senile plaques.** ApoE
1101 and Aβ staining in CAA (dashed lines, top two panels) and in a dense-core senile plaque
1102 (dashed lines, third panel) and in diffusive senile plaques (dashed lines, bottom five
1103 panels) was shown in this figure. ApoE and Aβ staining in diffusive senile plaques with
1104 different sizes showed highly variable ApoE intensities. Scale bar, 50 μm.
1105
1106
1107
1108
1109

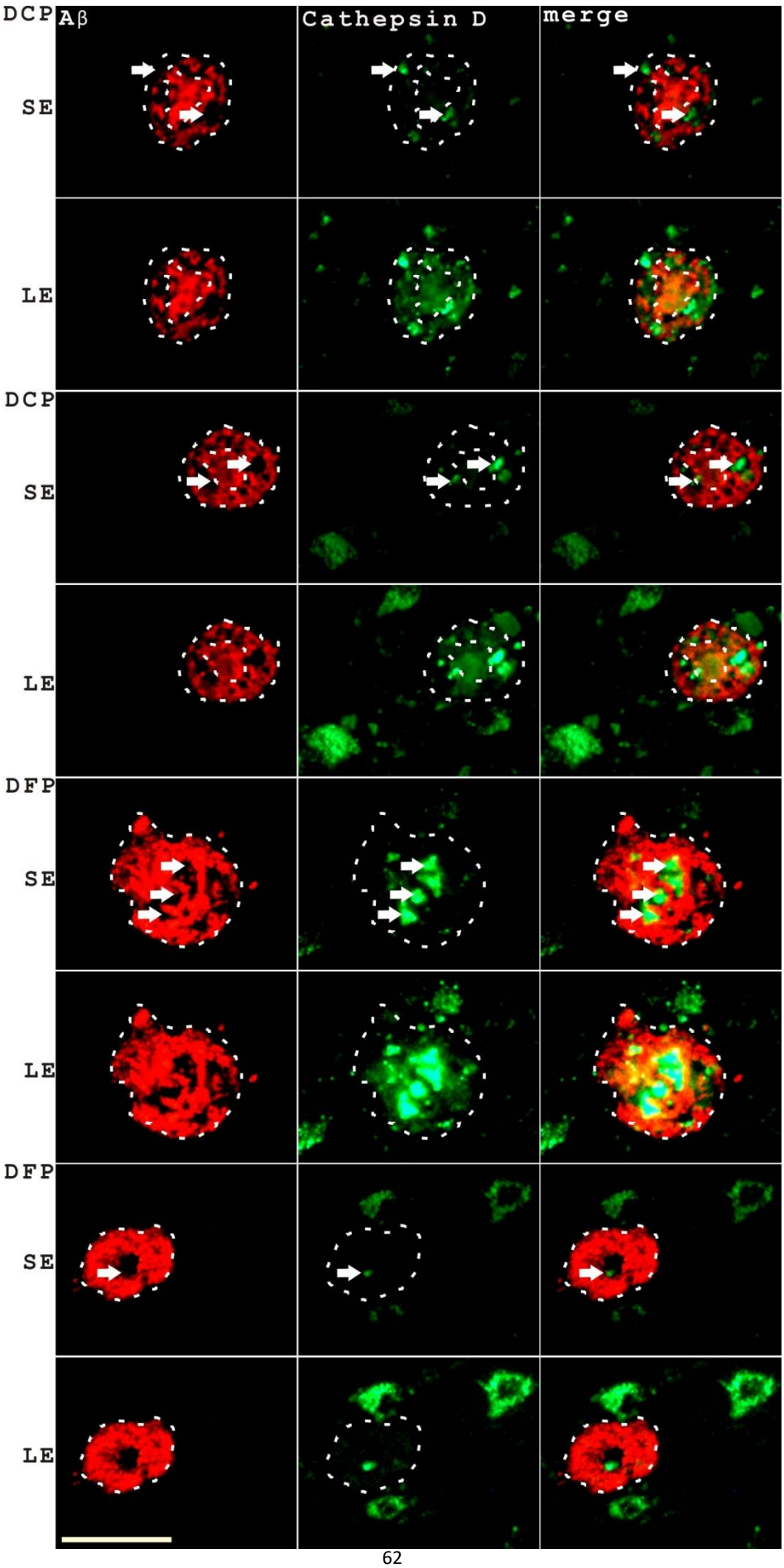

1110

1111 **Supplementary Figure 4. The two distinct layers of Cathepsin D expression in**
1112 **senile plaques were verified with another Aβ/Cathepsin D antibody pair.** Dense-
1113 core senile plaques showed two layers of Cathepsin D staining using two different
1114 exposure setting of the Cathepsin D staining were shown in the top four panels (SE
1115 stands for short exposure of 0.5 second while LE stands for long exposure of 1 second).
1116 A diffusive senile plaque with two layers of Cathepsin D staining was shown in the fifth
1117 and sixth panels. A diffusive senile plaque with very weak plaque Aβ-overlapping
1118 Cathepsin D staining was shown in the bottom two panels. The arrows pointed to the
1119 strong granule type of Cathepsin D staining while the dashed lines indicated the weaker
1120 but constitutive Cathepsin D staining overlapping with senile plaque Aβ staining. Scale
1121 bar, 50 μm.
1122